Modelling the kinetic of metallocenes during slurry phase homopolymerization of ethylene

Ana Cristina Gregório de Matos Oliveira

Thesis to obtain the Master of Science Degree in

Chemical Engineering

Supervisors: Prof. Dr.º Timothy F.L. Mckenna

Prof. Dr.ª M. Rosário Gomes Ribeiro

Examination Committee

Chairperson:	Prof. Dr.º José Manule Félix Madeira Lopes
Supervisor:	Prof. Dr.ª M. Rosário Gomes Ribeiro
Member of the committee:	Prof. Dr.º Carlos Manuel Faria de Barros Henriques

November 2014

Modelação da cinética de polimerização de etileno com catalisadores metaloceno em suspensão

Ana Cristina Gregório de Matos Oliveira

Dissertação para obtenção do Grau de Mestre em

Engenharia química

Supervisores: Prof. Dr.ºTimothy F.L. MCKENNA

Prof. Dr.ª M. Rosário Gomes Ribeiro

Júri :

Presidente:	Prof. Dr.º José Manule Félix Madeira Lopes
Supervisor:	Prof. Dr.ª M. Rosário Gomes Ribeiro
Vogal:	Prof. Dr.º Carlos Manuel Faria de Barros Henriques

Novembro 2014

Acknowledgements

I would like to start to thank to my supervisors from C2P2, Dr. Timmothy Mckenna , for giving me support and aid in my work, and also to phD student, M. Muhamed Bashir, to share the reactor with me and for the availability to answer all my questions and doubts.

I also want to thank to permanent staff from the laboratory for the help to manipulate the reactor, GPC and DSC analyses machines.

I want to show my gratitude to my IST supervisor Prof. Dr. Rosário Ribeiro for all the help and support especially the important advices for improve my work, even if it was by skype.

I would like to thank to my Portuguese friends that came with me also, especially to my residence neighbor Pedro. Also I would like to send a huge thank for all the friends and work colleagues that I met in France, for the help and good moments I passed in work and in Lyon, without you this would not have been a wonderful experience. I am especially grateful to my office colleagues, who shared the office during these months and always create a good work environment.

My friends at Portugal also deserve my thanks for even at the distance shared with me the good and bad moments of our academic pathway, especially to Bruna and Sónia. And also my boyfriend Pedro, for the support.

Finally, I could not forget my parents, for all their support and efforts all this years, and for always gave me the conditions to pursue my objectives.

Abstract

Recently, metallocenes immobilized on supported materials have been introduced as successful polymerization catalysts in industry. These catalysts have the advantage of unique control of polymer properties, thus making them ideal for the creation of new, application-oriented polymeric materials. Silica is one of the most used supports for metallocene heterogenization. However before anchoring the catalyst and/or cocatalyst, it is necessary a thermal treatment to remove residual water and hydroxyl groups from the support. The dehydroxylation temperature used effects the reaction of the support surface with the catalyst and thus the type of active centers formed .

The purpose of this work was to study and model the kinetics of ethylene polymerization catlyyzed by $(EtInd)_2ZrCl_2$ and $(n\text{-}BuCp)_2ZrCl_2$ metallocene catalysts supported on silica pre-treated at 3 different dehydroxylation temperatures. Results have shown that single site model comprising non-instantaneous activation and $1^{\underline{st}}$ order decay exhibits the best fitting to experimental kinetic data.
Then, to understand how the microstructure of the polyethylene produced, is affected by silica dehydroxylation temperature and reaction time, SEC analysis was used to determine the molecular weight distribution, MWD, of polymer chains. In addition, DSC was used to evaluate the crystallinity of the polymer formed. In order to characterize the multiplicity of active centers operating during polymerization, MWD curves of the polymer samples were analyzed and their deconvolution was performed assuming a Flory distribution. Results point out to the presence of 2 to 3 different active sites families that may change with time.

Keywords: Supported Metallocene, Modelling Kinetic, Dehydroxylation Temperature, Polymer Microstructure.

Resumo

A utilização a nível industrial de catalisadores metalocénicos imobilizados em suportes, para a polimerização de olefinas, apresenta como vantagem a possibilidade única de controlo das propriedades dos polímeros obtidos. Contudo, antes da imobilização é necessário efectuar um tratamento térmico prévio ao suporte (normalmente sílica) de forma a remover a água residual e grupos hidroxilo. Este tratamento afecta a reacção do suporte com o catalisador e consequentemente o tipo de centros activos formados.

O objectivo deste trabalho consistiu no estudo e modelação da cinética de polimerização de etileno usando os metalocenos $(EtInd)_2ZrCl_2$ e $(n\text{-}BuCp)_2ZrCl_2$ suportados em sílica submetida a diferentes temperaturas de desidroxilação. Os resultados mostram que o modelo que melhor se ajusta aos dados cinéticos é o modelo de activação não instantâneo com decaimento de 1ºordem.

Foi ainda estudado o efeito da temperatura de desidroxilação do suporte e do tempo de polimerização, na microestrutura do polímero nomeadamente foi determinada a distribuição de massas molares e a % cristalinidade do polímero. A fim de caracterizar a multiplicidade de centros ativos durante a polimerização, as curvas de distribuição de massas molares MWD foram analisadas e, efectuada a respectiva desconvolução tendo assumindo uma distribuição de Flory. Os resultados apontam para a existência de 2 ou 3 tipos de centros activos, dependendo das condições usadas, e que variam de intensidade e pesos moleculares ao longo do tempo de reacção.

Palavras-chave: Metalocenos suportados, Modelação cinética, Temperatura de desidroxilação, microestrutura do polímero.

List of symbols

$[C_0]$	initial concentration of active sites, mol/L
D_n	dead chain of length n
D_*	catalyst deactivated
I	impurities
P_n	polymer chain of length n
C_*	catalyst activated
F_A	monomer flow rate, mol/L
$[M_s]$	monomer molar concentration at the active sites in the polymer, mol/L
$[Y_0]$	total molar concentration of living chains or active centers in solution (heptane), mol/L
[C]	concentration of active sites in solution, mol/L
Vr	volume reactor, L
x_c	fraction of active sites in the catalyst system
wc	weight of the catalyst, g
M_m	molar mass, g/mol
ε	fraction of inicial active sites
z	compressibility factor
$[M]_g$	concentration of monomer in gas phase, mol/L
$[M]_l$	concentration of monomer in liquid phase, mol/L
K_{g-l}	gas-liquid partition coefficients apparent
K^*_{g-l}	gas-liquid partition coefficients apparent
P_M	partial pressure of ethylene, bar
K_{l-s}	liquid-solid partition coefficients
K^*_{l-s}	liquid-solid partition coefficients apparent
M_n	number average molecular weight
M_w	weight average molecular weight
M_i	molecular weight of a GPC cut
N_i	number of polymer molecules in a GPC cut
m_i	fraction of molar mass of each family of active sites
T_b	temperature in the balast, ºC
P_b	pressure of ethylene in the balast, bar
V_b	volume of balast, L
M_{Et}	ethylene mass in the balast, g
k_a	activation catalyst constant, min^{-1}
k_d	first-order deactivation, min^{-1}

k_d* second-order deactivation, $L.mol^{-1}min^{-1}$

k_p* propagation constant $L.mol^{-1}\ bar^{-1}min^{-1}$

T_b temperature in the balast (ºC)

P_b pressure of ethylene in the balast (bar)

V_b volume of balast (L)

M_{Et} ethylene mass in the balast (g)

List of acronyms

DSC differential scanning calorimetry

MAO methyaluminoxane

MWD molecular weight distribution

PDI polydispersity index

SEC size exclusion chromatography

TEA triethyaluminum

TCB tricholorobenzene

TiBA triisobutylaluminium

Contents

List of figures

List of tables

Introduction

Polyolefins are the largest group of thermoplastics, often referred to as commodity thermoplastics. The two most important and common polyolefins are polyethylene and polypropylene and they are very popular due to their low cost and wide range of applications.

At the heart of all polyolefin manufacturing processes is the system used to promote polymer chain growth. For industrial applications, polyethylene is made with either free radical initiators or coordination catalysts. Coordination catalysts, especially metalocene catalysts, can control polymer microstructure much more efficiently than free radical initiators and are used to make polyolefins with a wide range of properties.

Ethylene polymerization processes can operate with homogeneous catalysts in solution reactors or with heterogeneous catalysts in two-phase or three-phase reactors. Usually, olefin polymerization is carried out by using catalyst supported on porous supports. These catalysts are preferred in industry because they lead to well define polymer morphology and reduce drastically reactor fouling. The support also helps to maintain the particle integrity controlling better the microstructure.

Between all types of catalyst, heterogeneous metallocenes supported on MAO/ silica will be used in this work. By making a thermal treatment to Silica, the surface composition may be changed by controlling the type and proportion of the different groups, silanol and siloxane. During the heating water is removed in a first place (dehydration) then the hydroxil groups react forming siloxane groups that are desirable to react with catalyst. The temperature used in dehydroxydation procedure affects deeply the catalyst performance on reaction.

The main scope of this thesis is to understand how this temperature affects polymerization kinetics and to determine the main kinetic parameters of reaction. This way, different approximations, namely instantaneous or non-instantaneous site activation and first or second order deactivation, will be applied to a general model for the kinetics of single site catalysts. The fitting of the experimental data to the alternative models will allow to determine which model describes better the systems under study.

With respect to reactor phase, industrially is more common the gas phase mode, however for kinetic studies, in this case since the reaction is highly exothermic, it´s difficult to have a good control of temperature so usually is chosen slurry phase.

Supported catalyst present some heterogeneity resulting in multiple-site-type catalytic systems that typically exhibit broad molecular weight distribution (MWD). This behavior can be estimated by polydispersity index (DPI) which measures the heterogeneity of polymer chain sizes, given by the ratio between M_w and M_n.

Deconvolution of MWD is a new approach to identify the number of active site types and chain microstructures produced on each active site type.

The work developed under the scope of this thesis is organized in the following way,

In Chapter 1 the literature review will be presented. It comprises a general overview about the main polyethylene processes, a special focus on metallocenes and derived supported catalysts, and a brief description of the catalyst system used. The importance of the polymer microstructure and experimental techniques used to evaluate them is referred. Finally, the kinetic models for single site catalysts will be described.

Chapter 2 refers to experimental procedures done in the scope of this work

In Chapter 3 the results of the fitting of the experimental data, to the developed models for the two different supported catalyst types, n-$BuCp_2ZrCl_2$ and $EtInd_2ZrCl_2$, will be developed and the kinetic parameters evaluated. Additionally, the crystallinity and the MWD of polyethylene produced with each catalyst type will be analyzed and the results discussed.

The main conclusions are presented in Chapter 4.

Next, in Chapter 5 the Future Perspectives are discussed.

And finally Chapter 6 refers to Annexes.

Cap 1. Literature review

1.1 Polyethylene manufacture

Polyethylene (PE) resins are produced from ethylene gas. Ethylene gas is derived from the cracking of natural gas or petroleum by-products.

By using different reactor technologies such as operating multiple reactor configurations and combining other monomers such as vinyl acetate or other olefins (butene, hexene, octene) in conjunction with ethylene to form copolymers, we can produce many different types of PE resin. The ability to produce so many variations of a basic material permits the manufacturer to have PE resins for diverse applications, such as packaging films, rigid food containers, milk and water bottles, large toys, etc.

With respect to the reaction mechanism, polyethylene can be produced by free-radical polymerization or by catalyzed polymerization mechanisms using coordination catalysts. With the later method, the polymerization is carried out on a catalyst with a coordination insertion mechanism, in which the monomer units are inserted between the catalyst site and the growing polymer chain. Meaning that the catalyst has the control of insertion process, allowing the production of a polymer with a specific stereoregularity (ex. polypropylene). In free-radical polymerization, the active center is a reactive specie that is an electron donor, and polymerization proceeds by addition of monomer units on the active end of growing chain. The different insertion monomer mechanism creates more branched molecular structures in the case of free-radical initiators and more linear chains for coordination catalysts.

LLDP, LDP and HDP classification

Polyethylene is classified into several different categories based mostly on its density and branching. It´s mechanical properties depend significantly on variables such as the extent and type of branching, the crystal structure and the molecular weight distribution. With regard to sold volumes, the most important polyethylenes are HDPE, LLDPE and LDPE.

Low density polyethylene (LDPE) is normally produced by autoclave or tubular reactor technology by free radical polymerization at high pressures (around 1500-2500 bar) and temperatures (200-300°C). These extreme conditions are responsible for a constantly changing active site position in the growing polymer chain, resulting in a polymer with a random highly branched structure, as shown in Figure 1. The LDPE has low crystallinity and low density ranging from 0.915 to 0.935 g/cm^3. As a result of the low crystallinity, the end-use applications for this polymer type are flexible and soft materials. Typical applications include high-clarity film, flexible food packaging, heavy-duty films, caps and closures.

Linear low density polyethylene (LLDPE) is typically made by using a transition-metal catalyst in gas phase reactors at lower pressures (10-30 bars) and lower temperatures (70-90°C) compared with LDPE. Comonomers, such as butene, hexene or octene are added with ethylene to create linear polymer chains with short chain branches and low densities. Some typical applications include heavy-duty shipping sacks, industrial packaging, flexible food packaging, storage boxes and thin-wall lids.

High density polyethylene (HDPE) can be polymerized by using slurry, solution or gas-phase reactors. HDPE manufacturing processes also use transition-metal catalysts to make linear polymer chains with less branching than LLDPE. Polymerizing ethylene without any comonomer produces HDPE homopolymer. The resulting products exhibit the highest density and crystallinity in the PE family. Due to that, HDPE products tend to show higher stiffness, which makes them suitable for rigid packaging applications. HDPE market shows significant levels in blow molding, injection molding, and film. Typical applications consist of detergent bottles, milk bottles, pails, thin-wall containers, drink cups, cases and crates and grocery bags.

HDPE (low degree of short chain branching)

LLDPE (High degree of short chain branching)

LDPE (High degree of short and long chain branching)

Figure 1 – Polyethylene different classifications concerning branching

The choice between slurry, gas phase and solution technologies depends mainly on economic factors.

In slurry process, is used a diluent that is a nonsolvent for polyolefins to suspend the polymer particles. Due to high heat capacity, the diluent act as a heat removal. However, as a disadvantage, it requires removal, purification and recycle unit operations, which add extra costs. In addition the diluents that can be used in this process also dissolve amorphous PE, making it difficult to make LLDPE this way.

For gas phase, the main advantage regarding to slurry, is the absence of any solvent in the reactor, making inexpensive the separation between the solid and continues phase. However not having a solvent causes a heat removal problem because there are risks of hotspots and polymer agglomeration. At lab and pilot scale to work around the problem, it is usual to introduce solids that acts as diluents and promotes the heat removal. In industrial scale sometimes is added an “induced condensing agent” that evaporates and recondensed in a recycle stream, to help the heat removal. In gas phase only supported catalysts can be used.

The only reactor that can be used for gas phase polymerization of ethylene is the fluidized bed. It consists in a vertical cylindrical reactor in which particles are fluidized by the gas at enough velocity to keep the particles inside. The success of this reactor is in the effectiveness of heat removal due to the relatively high gas-particle velocities in the bed. For this type of reactors the use of a supported catalyst is essential.

On the other hand, solution process uses homogeneous catalyst and the reactor is operated at higher temperatures and pressures than slurry and gas phase. In order to maintain the polymer dissolved in the reactor medium. The non-supported active sites makes easier to overcome transfer mass resistances, making the reaction very fast. However, reactor fouling can be a real problem because the dissolved polymer can stick to the reactor walls. It also has the disadvantage of drying operation requirement by the fact of being in solution, which also reflects negatively on costs.

1.2 Coordination catalysts

There are four families of catalysts, Ziegler-Natta, Phillips, Metallocene and transition metal catalysts.

Philips and Ziegler-Natta were the first coordination catalysts to be used on a commercial scale. They have multiplicity of active sites, making polymers with nonuniform microstructures characterized by broad MWD. On the other hand, Metallocene and late transition metal catalyst are characterized by being single site, making polymers with more uniform properties resulting in narrow MWD.

The Phillips catalyst is one of the most widely-used supported catalysts for polyethylene, along with the Ziegler-Natta catalysts (named after the scientists who received the 1963 Nobel Prize for developing them). Both are commonly used in industrial application, but the Phillips catalyst is less expensive and less versatile in terms of the range of polyethylene types it can make. It was discovered in 1951 by Phillips Petroleum, when researchers attempting to make synthetic gasoline from natural gas over a nickel catalyst added a chromium promoter. The two researchers found the catalyst that would transform

ethylene and propylene into solid polymers, crystalline polypropylene and high-density polyethylene (HDPE), and this discovery gave rise to a whole new industrial process. [2]

The **Phillips catalysts** are only heterogeneous and are constituted of a chrome oxide (CrOx) or vanadium oxide (VOx) impregnated on silica. One of the main advantages of this system is that there is no need of activation agents because the catalyst is activated by the monomer. The products have a broad molecular weight distribution and the polydispersity index (PDI) can vary from 4 to 20.

Ziegler-Natta catalysts are composed of a transition metal salt of metals from the groups IV and VIII, for example, Ti is the most widely used. This type of catalyst needs a cocatalyst to activate it. The most commonly used are organometallic components of aluminum as TEA (triethyaluminum), TIBA (triIsoButylAluminum) and DEAC (DiEthylAluminumChloride). Unlike Philips, Ziegler-Natta catalysts can be heterogeneous or homogeneous. Homogeneous are vanadium-based. In heterogeneous type, the most common system used is $TiCl_4$ supported on $MgCl_2$ or SiO_2. This type of catalyst produces also broad molecular weights with PDI typically varying from 4 to 10.

The **Metallocene catalysts** were discovered in 1950´s, however, at that time they exhibited low activities and produced low molecular weight polyethylene [3]. Later it was found that a metallocene complex could reach very high activity when contacted with trimethylaluminium (TMA) precontacted with water. This was attributed to the reaction between water and TMA resulting in methylaluminoxane (MAO). Polyethylenes made with metallocene catalysts have a much more uniform microstructure from the ones with Ziegler-Natta and Phillips catalyst, with PDI around 2.

Late transition metal catalysts appeared in attempt to replace the free radical polymerization because the disadvantage of the use very high pressures. This catalyst type has a special feature which is the ability to “walk” along the growing polymer chain, leading to formation of short-chain branches (SCB’s). However, free-radical process is still currently the manufactory way to produce LDPE.

1.3 Metallocene catalyst

Metallocenes are composed of a transition metal atom sandwiched between two rings and two atoms of Chloride. The rings, also called ligands, can be connected through a bridge B in figure 2, which is responsible to vary the angle between the rings. In general they have the formula $Ring_2BMCl_2$, where B is the bridge between both rings, M is the metal and R represents other groups linked to the rings.

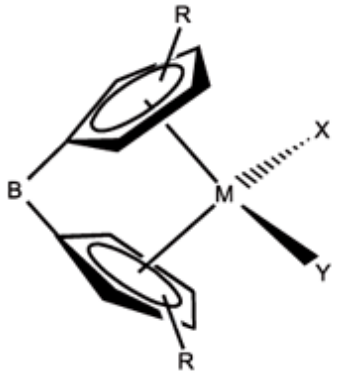

Figure 2 - basic structure scheme of metallocene Error! Reference source not found.

It´s possible to change the ligand type, type of bridge and type of transition metal atom.

A large variety of metallocene catalysts can be obtain by altering the simple structure of a zirconium base catalyst, as showed in figure 3.

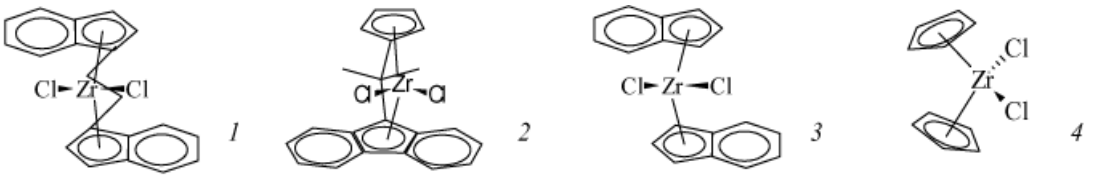

Figure 3 - Possible metallocene structures Error! Reference source not found.

Exists another type of metallocene called monocyclopentadienyl complexes, called often half-sandwich, which have just one ring.

By altering the electronic and steric environment around active sites it´s is possible to modify the accessibility and reactivity of the active sites resulting in polyolefin with different microstructures, although it´s not always easy to predict the result of a modification.

1.4 Supported catalyst

Despite the high polymerization activities, homogeneous metallocenes suffer some drawbacks like the lack of control of polymer morphology and reactor fouling. Therefore for the practical applications, the immobilization of metallocene compounds on a support is required. The key point is finding a way to anchor the metallocene onto the support without losing the advantages of homogeneous complex like high activity, stereochemical control and improved morphology required for industrial applications. The nature of support as well as the technique plays an important role in catalytic activity and polymer properties such as MWD.

Furthermore, studies on the morphology of the polymer indicated a direct relation between the polymer and support morphology as the support provides not only a way to supply the catalyst into the reactor, but also serves as a template for growing polymer particles. During polymerization, the particle shape is retained as the particle grows until fragmentation of the support. This phenomenon is therefore referred to as replication, and the particle size of the final polymer particle may be 20-50 times that of the catalyst support.

Figure 4 – The development of polymer particle growth during polymerization[5]

The most commonly used support for single-center catalysts are silica particles. Although silica is the most widely used support, other materials as alumina, Zeolites and others have been investigated, but they are not yet commercially useful as they lack activities similar to the ones of silica supported systems.

Silica exists in a number of crystalline phases but for catalyst support amorphous silica is normally used. This is by far the most common support used in the heterogenization of single-centre olefin polymerization catalysts, as it has high surface area and porosity, good mechanical properties and is stable and inert under reaction and processing conditions.

The properties of amorphous silica are mainly governed by the surface chemistry and specially by the presence and distribution of silanol groups. Three different types of silanol groups can be distinguished (a) geminal, (b) vicinal and (c) isolated [6]

Before the anchoring process, silica requires a thermal treatment to remove water and reduce the hydrogen bridges between silanol groups on the surface and leading to siloxane bridges. Hydrogen bonded water molecules need temperatures up to 180ºC. Up to this temperature the adjacent vicinal silanol groups condense with each other to form siloxane bridge which are desirable to react with MAO.

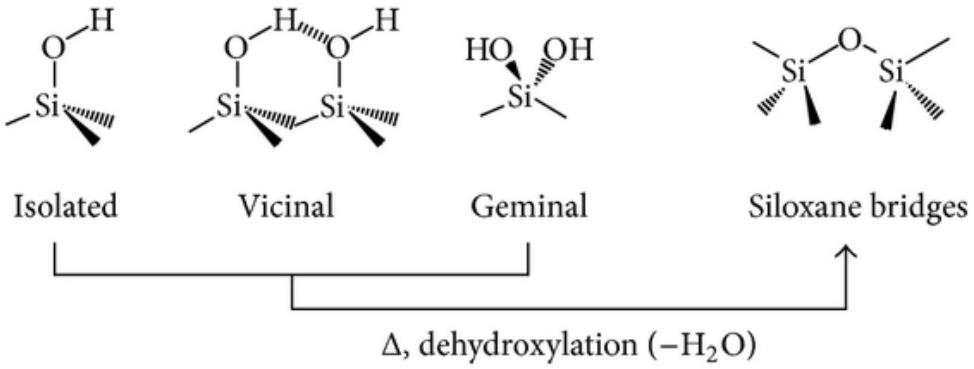

Figure 5 - partial dehydroxylation of the silica surface Error! Reference source not found.

The dehydroxylation temperature of the thermal treatment is usually chosen in order to remove residual water and hydroxyl groups, but it also depends on several factors such as the polymerization process, the supporting technique, and the cocatalyst and (pre)catalyst combination. The dehydroxylation temperature affects deeply the ability of the support to anchor the different species.

After silica thermal treatment, the cocatalyst (normally an aluminoxane) and (pre)catalyst are impregnated in the support.

There are three basic methods of supporting aluminoxane-activated single-site catalyst:

1. Supporting the aluminoxane and then reacting with (pre)catalyst
2. Supporting the (pre)catalyst and then reacting with aluminoxane
3. Contacting the aluminoxane and (pre)catalyst in solution before supporting

Method 2 consists in adsorbing the metallocene on the support and then reacting it with cocatalyst. In this method, the silanol isolated groups of silica, bond to chlorine of catalyst by via μ-oxo bonding. But if it still remains vicinal and germinal groups, when contacts with catalyst, there are a consume of the two chlorines in immobilization catalyst process as in (b) of fig 6, and as a result we have less active sites because the inadequate linkage between the support and metallocene.

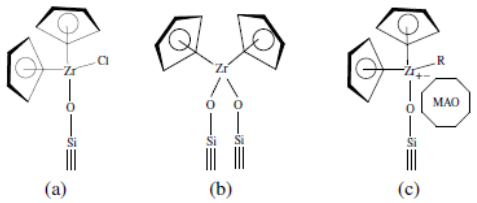

Figure 6 – Direct immobilization of metallocene on isolated (a) and vicinal (b) silanol groups of silica. Catalyst activated before MAO impregnation (c)

To prevent deactivation of these supported systems by reaction with silanol functionalities, it is common to use the first method, that chemically anchors the silica surface with an aluminoxane, in the present case, methyaluminoxane, known as MAO.

Supporting MAO first, followed by reaction with a metal complex, is the most frequently used and commercially available methods used to prepare heterogeneous single-center polymerization catalysts.

The dehydroxydated silica is precontacted with a toluene or with an aliphatic hydrocarbon solution of MAO followed by washing, drying and reaction with an appropriate catalyst precursor. To maximize the number of catalyst centers and reduce the volume of solvent, one can use the “incipient wetness” method, in which the support is contact with a minimum volume of metallocene and MAO solution volume

just to wet the solid support. The amount of Al/Zr is calculated in a form that is proportional to the pore volume.

Finally in method 3, the metallocene and the cocatalyst are precontacted before supporting

1.4.1 Catalyst system

The two catalyst studied in present case are (a) **Ethylenebis(Indenyl) Zirconium Dichloride -** $(EtInd)_2ZrCl_2$ and (b) **Butylcyclopentadienyl Zirconium Dichloride -** $(n\text{-}BuCp)_2ZrCl_2$

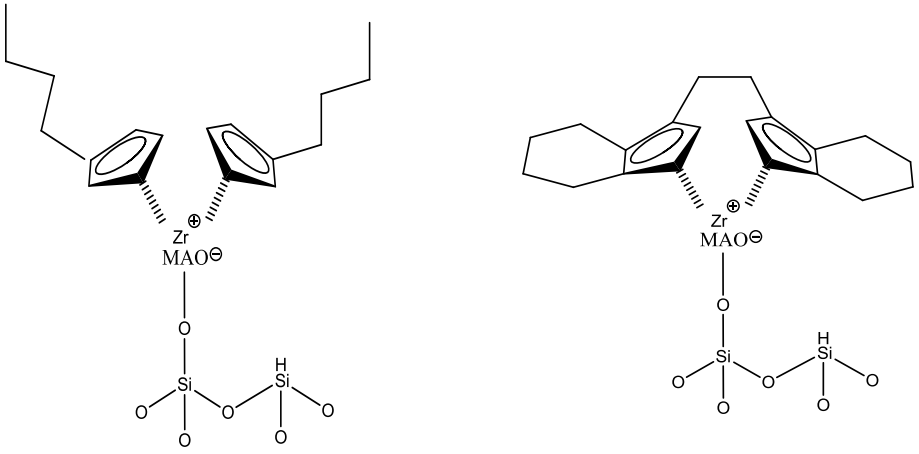

Figure 7 - Catalyst system (a) $(EtInd)_2ZrCl_2$ and (b) $(n\text{-}BuCp)_2ZrCl_2$ Draw with ChemBioDraw software

1.5 Polymer microstructural characterization

Since polyolefins are simply composed by carbon and hydrogen atoms, what determines the properties in case of homopolymerization, are the microstructure, which were evaluated in these case by molecular weight distributions and percentage of crystallinity.

MWD and crystallinity strongly influence the rheological and mechanical properties. In semi- crystalline polymers, the crystallization phenomenon plays also a crucial role in the quality of polymer.

SEC, size exclusion chromatography, is the most widely used technique for MWD determination. In this technique, polymer chains in a sample are fractionated using a series of columns packed with poly(styrene-divibylbenzene) gels with varying pore diameters. The polymer is dissolved in a solvent and separated according to their volumes in solution. The smaller chains follow into the most difficult path and penetrate deeper than the longer ones. That's why the first chains get out are the big ones.

On the base of the columns there are detectors. The more common detectors are refractive index (RI), infra-red (IR) and a viscosimeter (VISC). The disadvantage is that for all, it´s needed a calibration curve that relates the molecular weight with elution time or volume, as in figure 8. Sometimes with metallocene, polymers with some branching are obtained becoming more difficult to do this calibration because the elution time is not just related with molecular weight but also with branching density. And these curves are applied for linear polymers. For polymers with branching, all the detectors signals are taking into account, and we could get a molecular weight in absolute way and so there´s no need of a calibration curve.

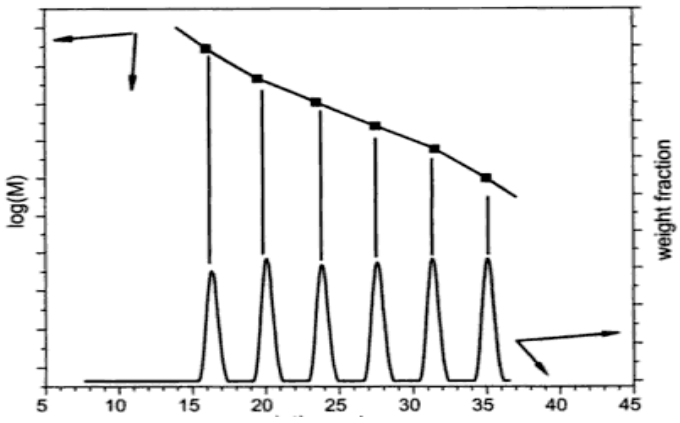

Figure 8 - Construction of the calibration line for the SEC Error! Reference source not found.

Once MWD has been determined, the molecular weight averages can be calculated using equations (1) and (2) respectively for the number and weight average molecular weight.

$$M_n = \frac{\sum M_i N_i}{\sum N_i} \qquad (1.1)$$

$$M_w = \frac{\sum {M_i}^2 N_i}{\sum M_i N_i} \qquad (1.2)$$

The polydispersity factor, that measures the heterogeneity of polymer chain sizes, is given by the ratio between Mw and Mn.

$$PDI = \frac{M_w}{M_n} \qquad (1.3)$$

To obtain the MWD distributions and deconvolution, refractive index (RI) data was exported from OmniSEC software. These RI values are the difference between refractive index n of a solution eluted at volume Ve and the refractive index n_0 of the solvent pure. The detector response is proportional to the weight of dissolved polymer.

Expanding the refractive index, n, in Tayler series as function of concentration C of the solution eluted at volume Ve, and neglecting the higher order terms of expansion, we have equation 1.4. [9]

$$n - n_0 = \frac{dn}{dC} \times C \qquad (1.4)$$

Where dn/dC is the increment which depends on the polymer type. The concentration C of the solution is proportional to the weight of the polymer dissolved. This implies that the refractive index detector measures the weight fraction of the same polymers chains as showed in equation 1.5

$$\frac{dC}{C} = \frac{dn}{n - n_0} \qquad (1.5)$$

Deconvolution

Since the catalyst is supported, several types of active sites with a different accessibility and reactivity are present, giving rise to polymer chains with different properties namely MWD.

The MWD obtained in SEC analysis can be a reflect of the contribution of each active sites type on the overall polymer microstructure. This way, it´s assumed that the overall MWD will be the sum of MWD of

each type of active site. In order to determine the number of active site types, their contribution and how they evolve along reaction, deconvolution model was used.

In this model chain formed on each active site type assumed to follow Flory´s distribution with PDI a fixed of 2 corresponding to single site typical PDI. The parameters are estimated with minimizing the sum of the squares of differences between experimental (SEC) and model data.

The MWD model deconvolution used is described in appendix 3.

With this model we could impose the number of families and compare which one fits better the experimental data. For each family assumed, we obtain a MWD curve with a specific Mw and Mn, as observed in example of MWD deconvolution of figure 9.

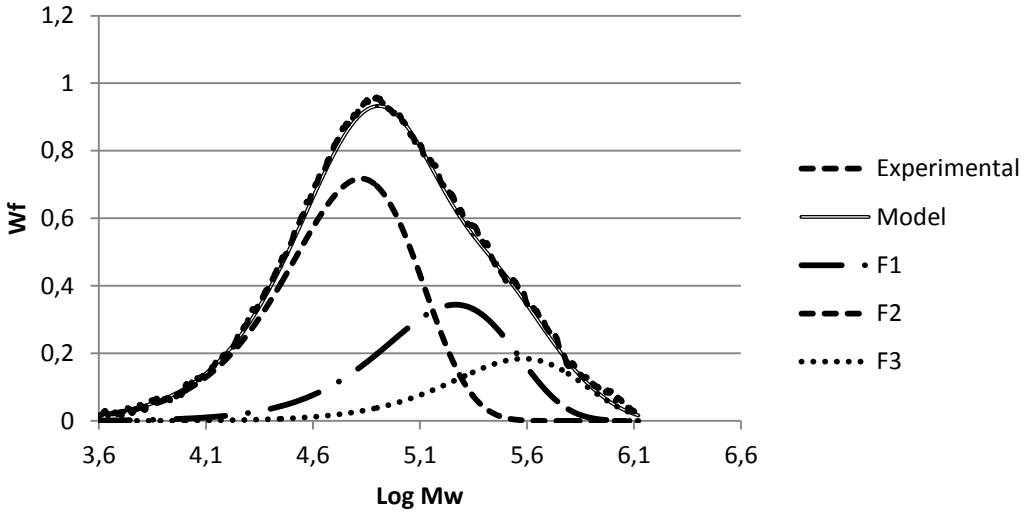

Figure 9 - Example of deconvolution of MWD SEC data into 3 families of active sites.

MW is normally in logarithm scale and the respective weight fraction, $w_{\text{Log Mw}}$, is given by equation 1.6.

$$w_{\log MW} = 2{,}3026 \times MW^2 \hat{\tau}^2 \exp(-MW\hat{\tau}) \qquad (1.6)$$

Where,

$$\hat{\tau} = \frac{1}{Mn} \qquad (1.7)$$

The global Mn and Mw, are the sum of all families of active sites, given by equation 1.8 and 1.9

$$M_n = \frac{1}{\sum \frac{mi}{M_{ni}}} \qquad (1.8)$$

$$M_w = \sum mi\ M_{wi} \qquad (1.9)$$

Crystallinity

Polyethylene is a semicrystalline material which can be considered as a composite of crystalline and noncrystalline regions. The noncrystalline phase, also called amorphous phase, forms a continuous matrix in which the crystalline regions are dispersed, as showed in figure 10.

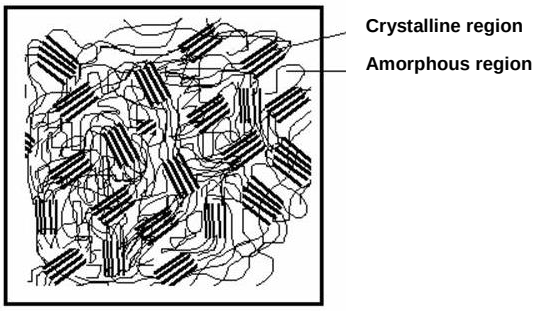

Figure 10 - Mixed amorphous crystalline macromolecular polymer structure.[24]

The specific morphology of the semicrystalline structure is governed by the molecular characteristics of the chains: the short-chains branching disturb the regularity of PE chain, and so they are responsible for a decrease of degree of crystallinity. For example, HDPE, with a little or no branching, has bigger crystallinity, in the range of 60-85%. On the other hand, LDPE and LLDPE, with more and longer-chain branches, have less crystallinities, with values around 40-60%.[23]

One of the methods to measure polymer crystallinity is Differential Scanning Calorimetry (DSC). This equipment is designed to measure the amount of heat absorbed from sample when submitted to a linear increase of temperature as a function of time. DSC contains two pans, one the reference pan that is empty and the other containing the polymer sample. Both are heated at the same rate. The amount of extra heat absorbed by polymer sample is the heat absorbed by the pan material given by the empty pan reference.

From DSC we can obtain the crystallization temperature, Tc, where polymer gives off huge heat to break hard crystalline arrangement and the melting temperature, Tm, where polymer completely loses its orderly arrangement. Crystallinity is calculated using as a reference the value of 293 J/g for 100% crystalline polyethylene.

1.6 Kinetic models

A complete process of modelling is very complex and involves not only the microscale, but also the mesoscale and macroscale. Macroscale(>1 m) takes into account the modelling of hydrodynamics inside the reactor.

In mesoscale (> 10^{-3} – 10^{-2} m) is modelled the temperatures and monomer concentration gradients in interparticle,intraparticle and particle-wall. At this scale these gradients depends on the size, porosity and structure of the catalyst and on the concentration of polymer created inside the particle, which interfere with the growing of polymer chain.

At microscale, is modelled the phenomena´s that occur at the catalytic active sites, like diffusion of monomer in micropores and polymerization kinetics. This phenomena's affect the microstructure, namely MWD and long and short chain branching. In the present case, only microscale will be considered, this means that after **achieving the stationary state, the kinetic is the limiting step regarding to mass transfer resistances.**

The strategy for creating a mathematical model that describes the behavior of homopolymerization kinetics is to find out first all the possible reactions that occur in the reactor mixture and then develop a population balance equation for each component.

1.6.1 Mechanism

The main steps in coordination polymerization mechanism include activation, propagation, transfer and deactivation.

Starting with activation, metallocene catalyst need some time to be activated inside the reactor.

$$\mathrm{C} \xrightarrow{ka} P_0 \qquad (2.0)$$

After activation, the polymer chain length grows with monomer insertion as described in the equation 2.1, known as propagation step.

$$P_n + M \xrightarrow{kp} P_{n+1} \qquad (2.1)$$

Since there is no H_2 in the feed, under the experimental conditions used in this work, there is no transfer to chain-transfer agent neither beta-hydride elimination to H_2.

H_2 is sometimes used as a chain-transfer agent to control the molecular weight of the polymer and get broader distributions.

However chain transfers to monomer during polymerization, leading to a vinyl-terminated chain, may occur.

$$P_n + M \xrightarrow{ktm} P_1 + D_n \quad (2.2)$$

In deactivation step, the catalyst, can deactivate naturally by mono or bimolecular mechanisms

$$C_* \xrightarrow{kd*} D_* \quad (2.3)$$

We could also have other deactivation pathways due to the fact of coordination catalyst being very sensitive to impurities and it can deactivate leading with the formation of an inactive site, D_* (Equation 2.5). The impurities can also stop the polymer chain to grow as in equation 2.4.

$$P_n + I \xrightarrow{kdi} P_n + D_* \quad (2.4)$$

$$C_* + I \xrightarrow{kdi*} D_* \quad (2.5)$$

1.6.2 General Model of kinetics single site [8]

In single site models, only activation, propagation, and polymer deactivation are considered.

The polymerization rate, Rp is given by the equation 2.6.

$$R_p = -\frac{d[M]}{dt} = k_p[M_s][Y_0] \quad (2.6)$$

In this case we have a semibatch reactor, so the polymerization rate can be equal to the monomer feed divided by the volume of the reactor, meaning that all the ethylene that enters in the reactor is consumed by the reaction.

$$R_p = \frac{F}{V_r} \qquad (2.7)$$

The balance of active sites in the reactor is given by equation 2.8

$$\frac{d[C^*]}{dt} = -k_a[C^*] \;\; (=) \;\; [C^*] = [C_0]e^{-k_a t} \qquad (2.8)$$

The initial concentration of active sites in the reactor for heterogeneous catalysts is given by the molar fraction of catalyst.

$$[\mathrm{C_0}] = \frac{\mathrm{x_c\, W_c}}{\mathrm{M_{m_c}}} \qquad (2.9)$$

Knowing that 1 mole of Zr is equivalent to 1 mole of catalyst $(n\text{-BuCp})_2ZrCl_2$ or $(EtInd)_2Cl_2$) we can calculate the fraction of catalyst moles knowing the Zr (wf) content (g/100g of total supported catalyst) obtain by elemental analysis.

$$x_c = \frac{Zr\ (wf)\ \times M_m\ (cat)}{M_m(Zr)} \qquad (3.0)$$

Initial Active sites

Despite having a mass of catalyst with a molar number of active sites determined by elementary analysis, only a small fraction of active centers is active. This value is around 10% (ε) [8]

$$\left[\widetilde{\mathrm{C_0}}\right]_{(\mathrm{t=0})} = \varepsilon \times [\mathrm{C_0}] \qquad (3.1)$$

Concentration of monomer in the polymer

Since we are considering the concentration of monomer in the polymer and it´s a slurry semibatch reactor, we have a gas-liquid and solid phase, so it needs to be considered the gas-liquid and gas-solid monomer concentration. To simplify the problem some assumptions are taking into account.

- The concentrations in both phases are in equilibrium. Since the reactor is semibatch with continuous ethylene feed to keep the pressure constant, there is no variation of concentration of monomer if the equilibrium is achieved.
- It was assumed a linear relationship between concentrations in two phases using partition coefficient in respect/in terms of monomer partial pressure.

$$[M]_g = z\frac{P_M}{RT} \quad (3.2)$$

$$[M]_l = K_{g-l}\, z\frac{P_M}{RT} = K^*_{g-l}P_M \quad (3.3)$$

$$[M]_s = K_{l-s}\,[M]_l = K_{l-s}K^*_{g-l}P_M = K'_{g-s}P_M \quad (3.4)$$

Since we don´t know K´g-s, will be calculate an apparent kinetic rate constant, k^*_p.

The general rate equation will became as in equation 3.5

$$R_p = k_p K'_{g-S}P_M = k^*_p P_M \quad (3.5)$$

1.6.2.1 Instantaneous activation single site models

1.6.2.1.1 Model of First order deactivation with instantaneous activation

Given the general model presented before several approximations may be considered such as: instantaneous or not instantaneous site activation and first or second order deactivation.

In this section the dependence of Rp with time for instantaneous activation and first order deactivation will be developed

The balance to the total molar concentration of living chains $[Y_0]$, is given by equation 3.6.

In instantaneous mode, catalyst activation ka, which is the constant activation of catalyst for reaction, is zero due to the fast reaction start.

$$\frac{d[Y_0]}{dt} = k_a[C^*] - k_d[Y_0] \qquad (3.6)$$

=0

solving equation 3.6 simultaneous with equation 2.6 for initial condition of $[Y_0](t=0)=\widetilde{[C0]}$,we obtain the following solution.

$$\mathrm{Rp} = k_p{}^* P_M \varepsilon [\mathrm{C}_0] \mathrm{e}^{-\mathrm{kdt}} \qquad (3.7)$$

For the first order decay kinetics and instantaneous site activation, the logarithm of polymerization has to be a linear function of time. So if experimental data does not show a linear correlation between Rp and time, it means that this is not the operating mechanism for the tested conditions.

$$Ln\ R_p = Ln\left(k^*{}_p P_M \varepsilon [\mathrm{C}_0]\right) - k_d t \qquad (3.8)$$

1.6.2.1.2 Model Second order deactivation with instantaneous activation

The only difference between this model and the previous is that the deactivation result from a bimolecular deactivation mechanism. And so equation 3.6 turns into equation 3.9, with exponent 2.

$$\frac{d[Y_0]}{dt} = -k_d{}^*[Y_0]^2 \qquad (3.9)$$

Solving the equation 3.9 and considering $[Y_0](0)= \widetilde{[C0]}$, we obtain equation 4.0.

$$[Y_0] = \frac{\varepsilon[C_0]}{1 + \varepsilon[C_0]k_d{}^* t} \qquad (4.0)$$

Equation 4.0 is solved simultaneous with equation 2.6 for the same initial condition. Following the same development done for 1th order deactivation model we can obtain a linear relation between 1/Rp and time.

$$\frac{1}{Rp} = \frac{1}{k_p{}^* P_M \varepsilon [C_0]} + \frac{k_d{}^*}{k_p{}^* P_M} t \qquad (4.1)$$

1.6.2.2 Non-instantaneous single site models

1.6.2.2.1 Model First order deactivation with non-instantaneous activation

For first order deactivation without instantaneous activation, the system of equations to solve is the following.

$$\frac{d[C]}{dt} = -k_a[C^*] \quad (=) \quad [C^*] = [C_0]e^{-k_a t} \qquad (4.2)$$

$$\frac{d[M_s]}{dt} = -k_p{}^* P_M [Y_0] \qquad (4.3)$$

$$\frac{d[Y_0]}{dt} = (k_a)[C^*] - kd[Y_0] \qquad (4.4)$$

1.6.2.2.2 Model of second order deactivation with instantaneous activation

For second order deactivation model the set of equation to be solved, comprise the previous set of equations, where equation 4.4 was replaced by equation 4.5.

$$\frac{d[Y_0]}{dt} = (k_a)[C^*] - kd^*[Y_0]^2 \qquad (4.5)$$

To solve these differential equations the numerical solution Runge-Kutta 4 order was used (in appendix 1)

In the following sections these models will be used to fit the experimental kinetic data obtained for the catalytic systems studied, in order to determine which type of activation and deactivation model operates.

Cap 2. Experimental part

2.1 Manipulations

2.1.1 Preparation of supported catalyst

Dehydroxylation of silica

Silica (Grace 948) is introduced in a Schlenck tube and placed under vacuum and then is dehydroxynated using the temperature program of figure 11.

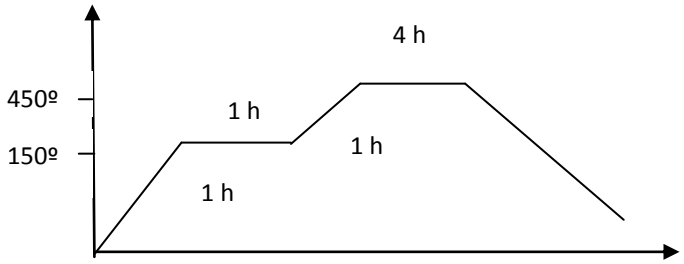

Figure 11 - Dehydroxydation Temperature program for 450ºC

There was used three dehydroxydation temperatures (200ºC, 450ºC and 600ºC.)

Impregnation of SMAO (silica+ MAO) and reaction with the catalyst

2 g of silica treated are introduced with a solution of MAO in toluene (30%) in a flask equipped with mechanical agitation under argon. And remain during 4 hours at 80ºC. The suspension is finally washed with toluene and the residual solid is dried under vacuum.

SMAO is suspended with the catalyst in hot toluene in a flask equipped also with agitation and under argon. The amounts of MAO and metallocene were calculated in the way to have an Al/Zr molar ratio of 150. The mixture is stirred at 50ºC during 1 hour. After the reaction the solid is again washed with toluene and then dried under vacuum. The catalyst system result is a yellow-orange powder for the case of $(EtInd)_2ZrCl_2$ (figure 12) and white for $(n\text{-}BuCp)_2ZrCl_2$.

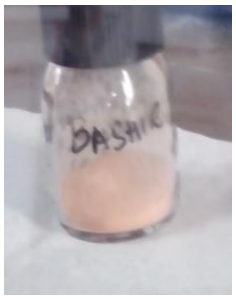

Figure 12 - $(EtInd)_2ZrCl_2$ powder used in experiments

The catalysts prepered in this work were calcinated at different temperatures for each type of catalyst showed in the tables 1.

Table 1 - Dehydroxydration temperatures

First serie of catalyst		
Et(Ind)2ZrCl2	**450º C**	**600ºC**

Second serie of catalyst			
(n-BuCp)2ZrCl2	**200ºC**	**450ºC**	**600ºC**

2.1.2 Polymerization technique – slurry in semibatch reactor (with continuous feed of ethylene)

The reactor used in this experiment is a 2,5 L reactor in steel with an spherical shape called turboshefere. Is equipped with a three blade stirrer and a four entries, one for argon and monomer entry, one used for the vacuum and also exhausted air, and another for the entry of the mixture, as showed in figure 13. The temperature is controlled by a jacket around the reactor with water circulating either for cooling, either for heating (with water from a warm bath). The stirring have also a refrigiration cooling system with water circulating.

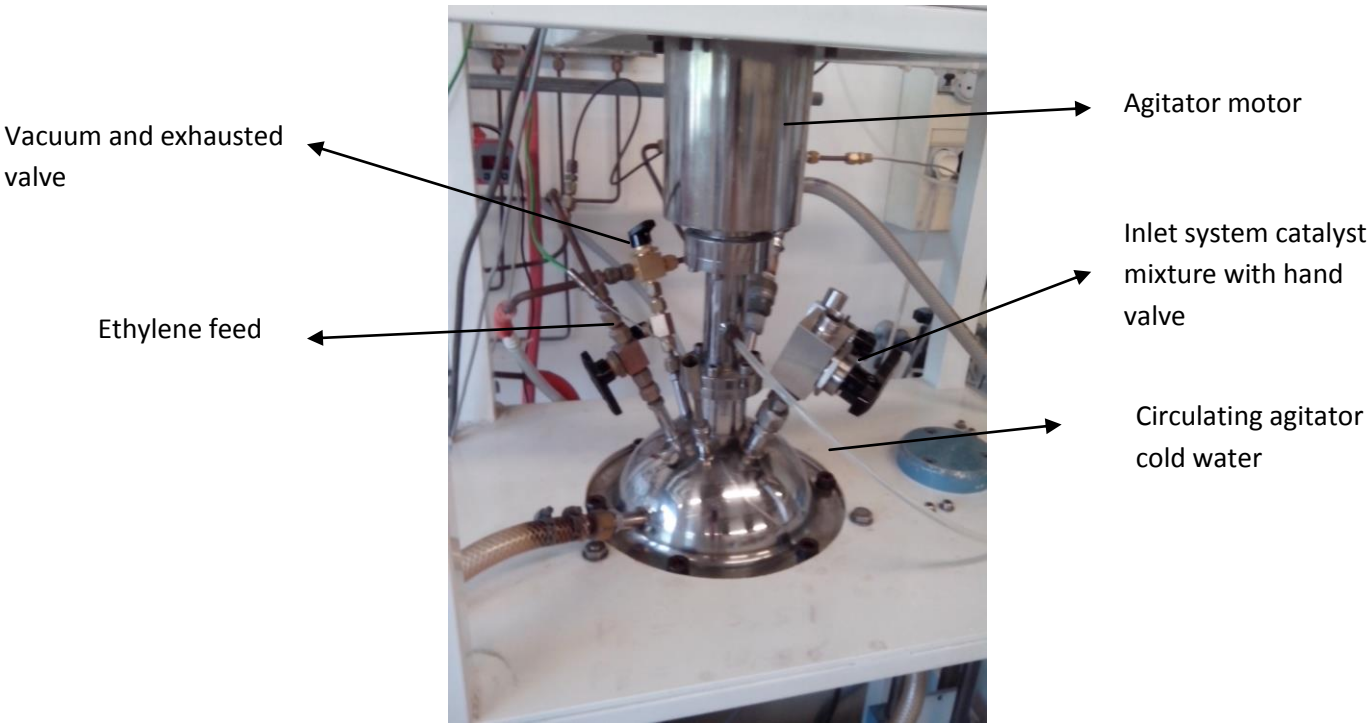

Figure 13 - Reactor used for experiments

Before starting a reaction, the reactor needs to be heat up to 80ºC and filled with argon and then vacuum three times during at least 1 hour. These cycles are made in order to clean the impurities inside the reactor. The same precedure is made in the 2-neck Schlenk, (a) fig. 14, that contain the reaction mixture.

After cycles proceed, this 2-neck Schlenk is filled with 500ml of heptene (diluent) and 1 ml of solution TiBA in heptane (1M). The purpose of **heptene i**s to facilitate the **removel** of heat transfer from the reaction since it is very exotermic. TiBA acts as a scavanger and clean all the remain impurities in the flask and heptane.

In a glove box, (b) fig 14, is placed an amout of catalyst (preferably the same amount each batch) in a small two-neck Schlenk. Experiments were done in the glove only when concentrations of oxygen were below 20 ppm.

The two flasks with catalyst and heptane were maintained into argon atmosphere and mixed each other with help of a thin tube and by changing argon pressure inside flasks.

Figure 14- two-neck Schlenk (a) and Glove box (b) used during experiments

After that, the mixture is injected into the reactor meanwhile cooled and the stirring speed adjusted around 350 rpm.

At last, the reactor is heated again to 80ºC and after reach this temperature, the monomer valve is open to handle a total pressure of 9 bar (8 bar of ethylene + 1 bar of argon), to start the polymerization.

The starting point of the reaction is when ethylene started to be consumed and we see a decrease in ethylene presure in the ballast. After that it is taken mesures of the pressure inside the ballast (controled by a monometer spy) every minute.

Once the reaction is finished the monomer inlet is closed and the reactor is rapidly cooled down and depressurized with exahusted outlet mouth. To recover the polymer, the reactor is open with an hydraulic sytem and then cleaned with heptane. To get the powder, the heptane-polymer is filtrated into a vacuum filter and then dryed in a vacuum chamber to remove the remains of diluent.

All the experiments performed and the respective reactor conditions are in a table in [appendix 2]

Figure 15- polyethylene looking after reaction in the reactor and after dried

How to calculate the activity

Since there is no flowmeter to measure the flow of ethylene, which corresponds to the amount of uptake monomer consumed in the reaction, the calculation of the activity was based on the measure of the PE pressure in the ballast of along time.

To convert pressure data in mass of ethylene, was used the following equation 4.6 instead of ideal gas law. This equation is an interpolation by parabolic regression of experimental data obtained by a phD student of the laboratory. The details of this mathematical regression are in appendix 6.

$$M_{Et} = V_b \times P_b \times ((1{,}256 - 0{,}004505T_b + 0{,}0000109{T_b}^2) + (0{,}0052 - 0{,}00001495T_b - 0{,}0000001244{T_b}^2)P_b + (0{,}0003252 - 0{,}00000732T_b + 0{,}00000004195{T_b}^2){P_b}^2) \quad (4.6)$$

By knowing the mass of Ethylene consumed along time and catalyst mass, it was possible to calculate the activity profile for each reaction.

$$Activity = \frac{\Delta m_{Et}\ (kg\ or\ g)}{\Delta \text{t (h or min)} \times m_{cat}(g)} \quad (4.7)$$

Since the experimental data obtained have a lot of noise, the calculation of activity which is given by the differential of mass dividing by a differential of time in equation 4.7, amplifies this noise resulting in activities with a lot of fluctuations. To reduce this problem, the experimental ethylene pressures were adjusted to an equation to get better activity profiles.

The Equation that best fits the experimental ethylene pressure was obtained in OriginLab software, and is given by equation 4.8. This equation comes from Logistic function, appendix 4

$$Pressure\ (bar) = A_2 + \frac{(A_1 - A_2)}{1 + (\frac{t}{X_0})^p} \quad (4.8)$$

2.2 Analytical techniques

2.2.1 Size Exclusion Chromatography (SEC)

SEC equipment (Viscotek) is composed by a series of 3 columns packed with poly(styrene-co divinylbenzene) gels with different pores diameter, where samples of polymer in trichlorobenzene (TCB) flows into these columns at a flow rate of 1Ml/min. In order to make sure that polymer chains are completely dissolved in TCB, the samples were placed at 150ºc for 3 hours. temperature.

The equipment gives the concentration of polymer in TCB by three types of detectors, refractomer, viscometer and infrared.

Figure 16- SEC analysis equipment and samples

2.2.2 DSC

The crystallinity and melting temperatures of the polymer were measured by DSC. In the preparation procedure, the samples of polymer were placed in holders with 40 µm. The quantity of polymer should be between 5 and 10 mg. Than the sample is placed in DSC holders showed in figure 17.

Two heating steps were performed, one from 20 to 180ºC at heating rate of 10ºC/min followed by a cooling from 180ºC to 20ºC at the same heating rate, and a second heating again 20ºC to 180ºC with some heating rate.

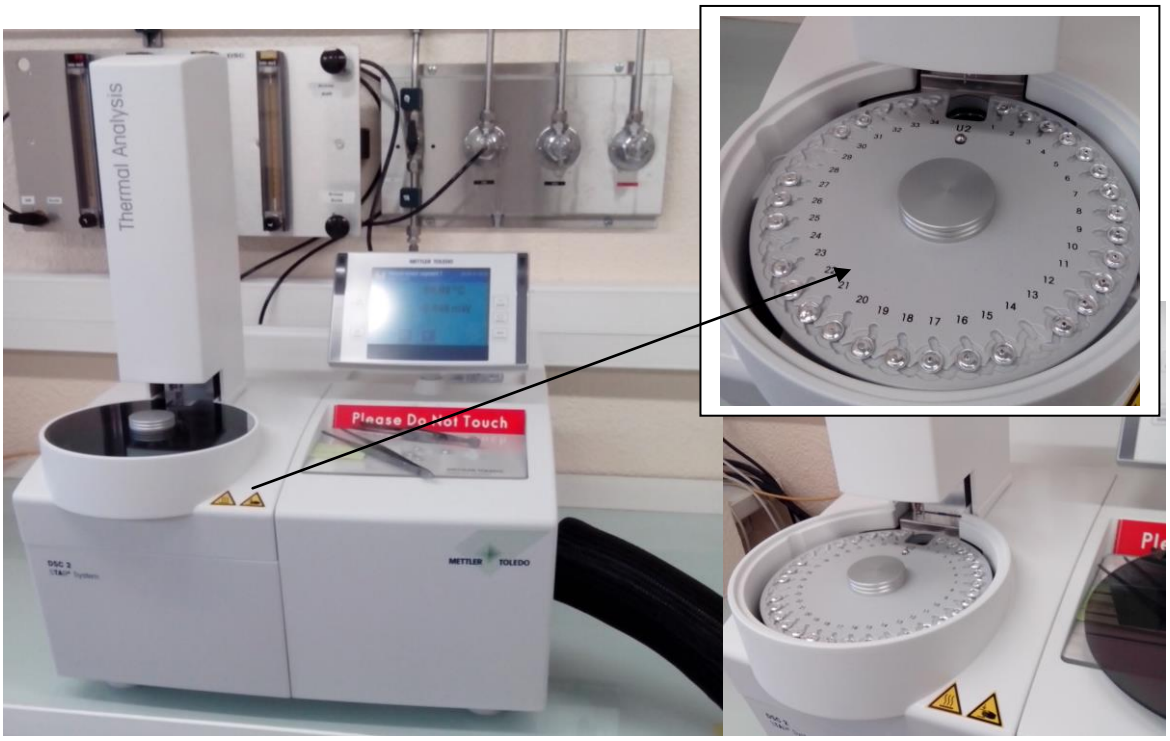

Figure 17- DSC equipment and placement for the samples

Cap 3. Results and discussion

3.1 Activities

Since the experimental data obtained have a lot of noise, the pressure data were adjusted to Logistic equation (mentioned above). Is it possible to observe in appendix 4, the results obtained with origin software of fitting logistic equation (red line) with experimental pressures in the ballast (black points). We can conclude by the R-Square´s values that this equation fits well the data. And so as a result the calculated activities, without noise, are showed in next graphics.

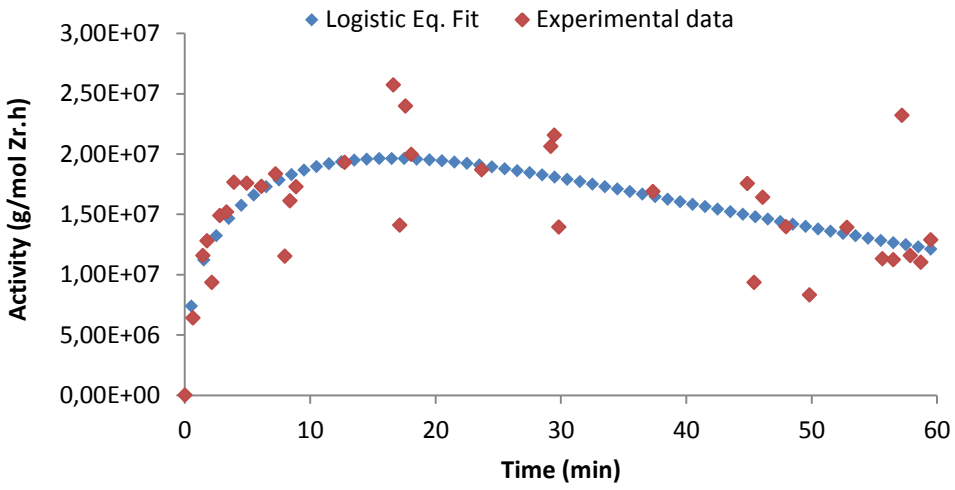

Figure 18 – Activities obtained for $(EtInd)_2ZrCl_2$ /SMAO (ANA_42 sample) at 450ºC dehydroxydation temperature

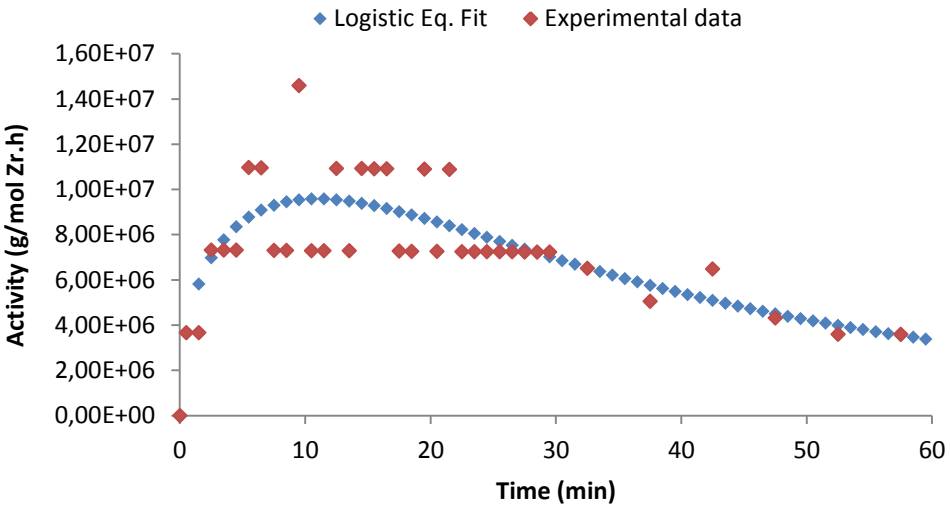

Figure 19 – Activities obtained for $(EtInd)_2ZrCl_2$ /SMAO (ANA_24 sample) at 600ºC dehydroxydation temperature

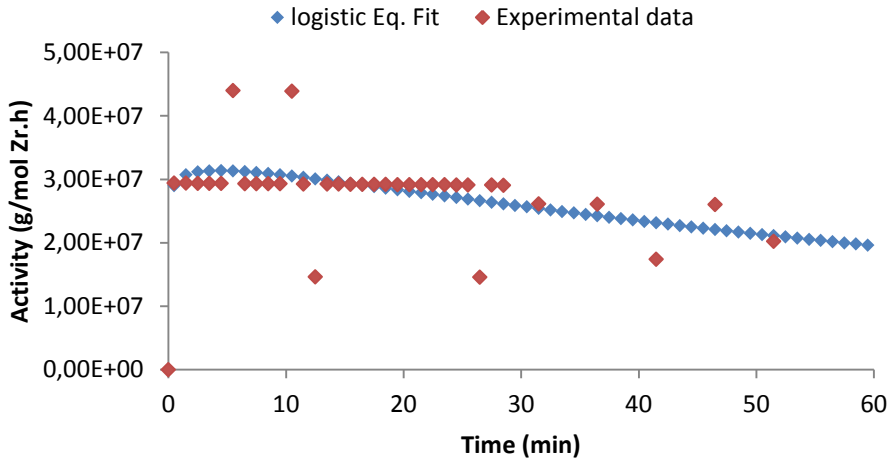

Figure 20 – Activities obtained for $(n\text{-}BuCp)_2ZrCl_2$ /SMAO (ANA_34 sample) at 200ºC dehydroxydation temperature

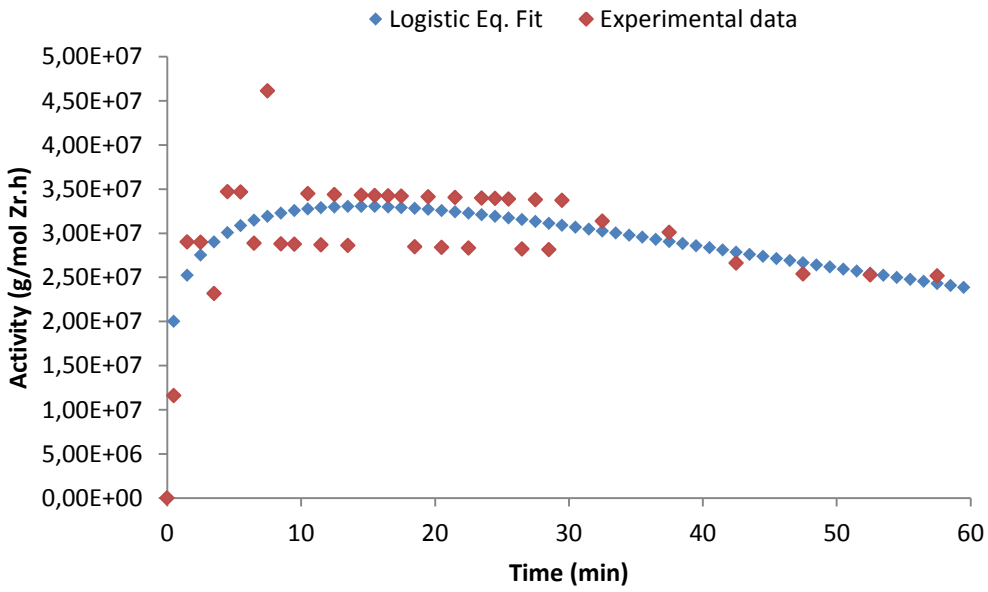

Figure 21 – Activities obtained for $(n\text{-BuCp})_2ZrCl_2$ /SMAO (ANA_27 sample) at 450ºC dehydroxydation temperature

For all the curves, it is noticeable that there is an initial max, from where activity starts to decrease, meaning that there are some deactivation.

In terms of industry concerns, it is more important to report the activities per gram of catalyst instead of mole Zirconium, because the amount of catalyst is important in terms of costs.

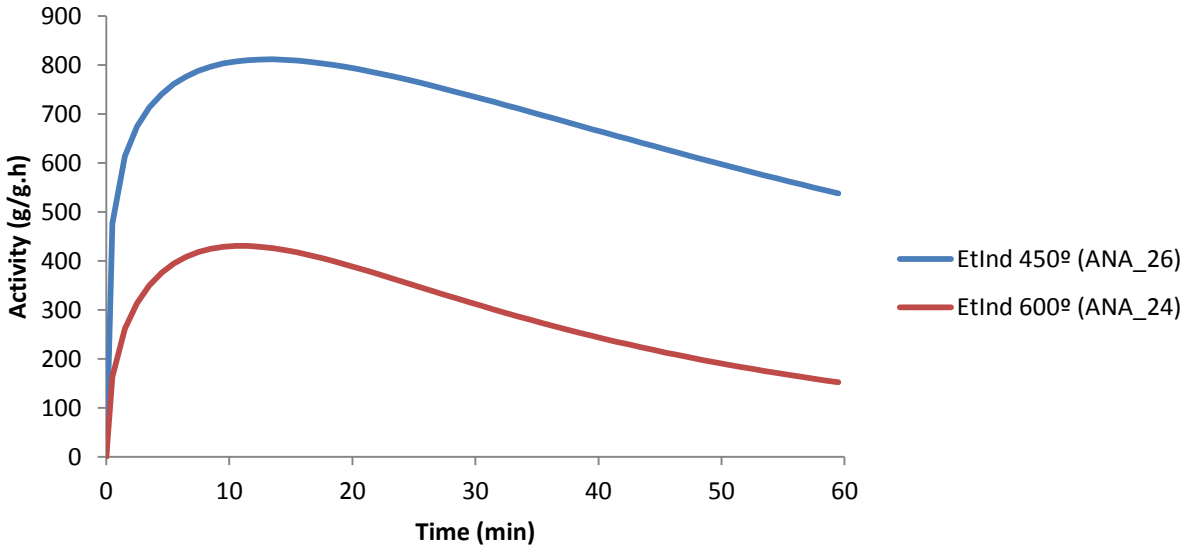

Figure 22 – Activities in g/g.h obtained for $(EtInd)_2ZrCl_2$ /SMAO series

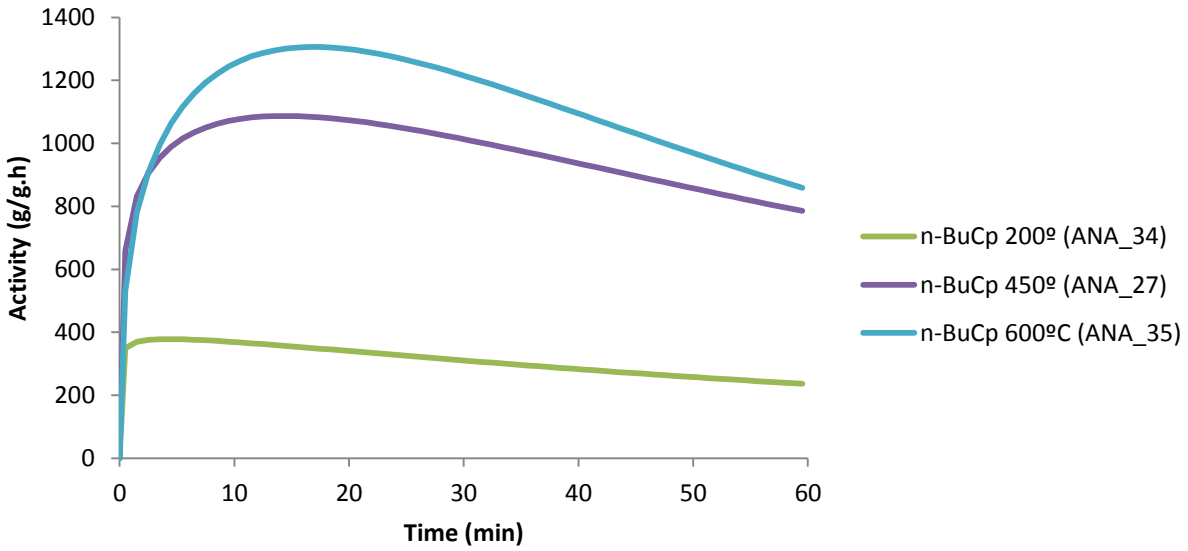

Figure 23 – Activities in g/g cat.h obtained for $(n\text{-BuCp})_2ZrCl_2$ /SMAO series

For the first catalyst series ($EtInd_2ZrCl_2$), we can observe that the activity is higher as lower is the dehydroxydation temperature, and so the maximum activity is achieved for 450ºC. The opposite happens with the second catalyst series $(n\text{-BuCp})_2ZrCl_2$), the activity increases as higher is the temperature, the highest activity being achieved at 600º C.

3.2 Instantaneous model results

The linearized equation for instantaneous activation models with 1st order and 2nd order deactivation are shown respectively in equation 4.9 and equation 5.0.

$$Ln\ R_p = Ln\left(k^*_p P_M\right) - k_d t \qquad (4.9)$$

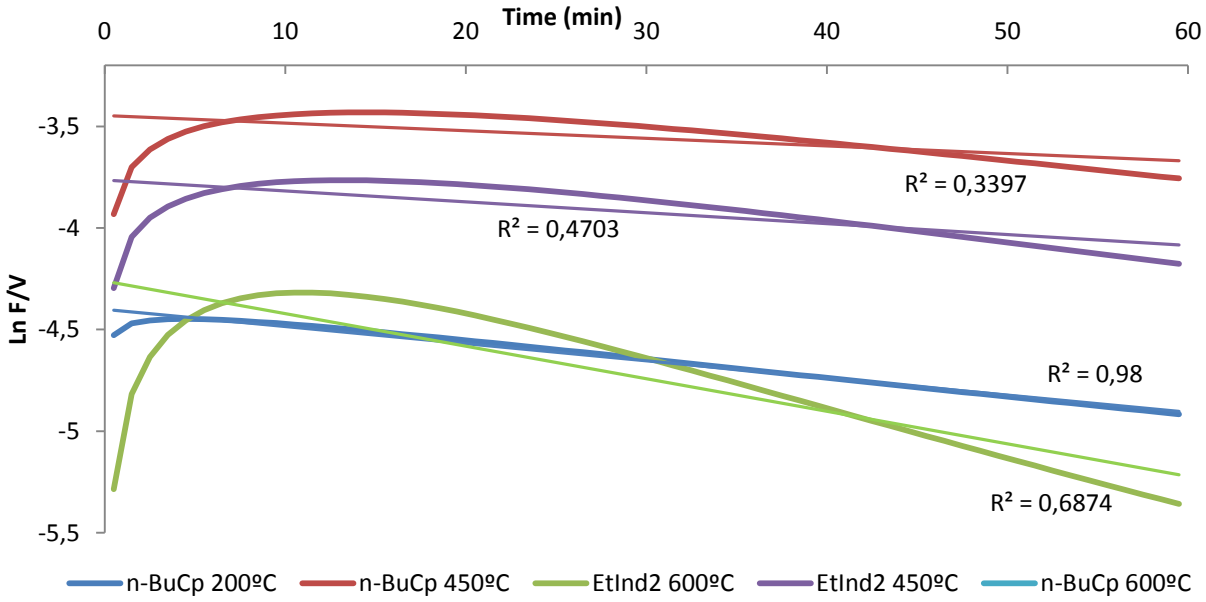

Figure 24 – Results of experimental data linearized and respective correlation line given by instantaneous activation 1st order decay model

$$\frac{1}{Rp} = \frac{1}{k_p{}^* P_M [C_0]} + \frac{k_d}{k_p{}^* P_M} t \qquad (5.0)$$

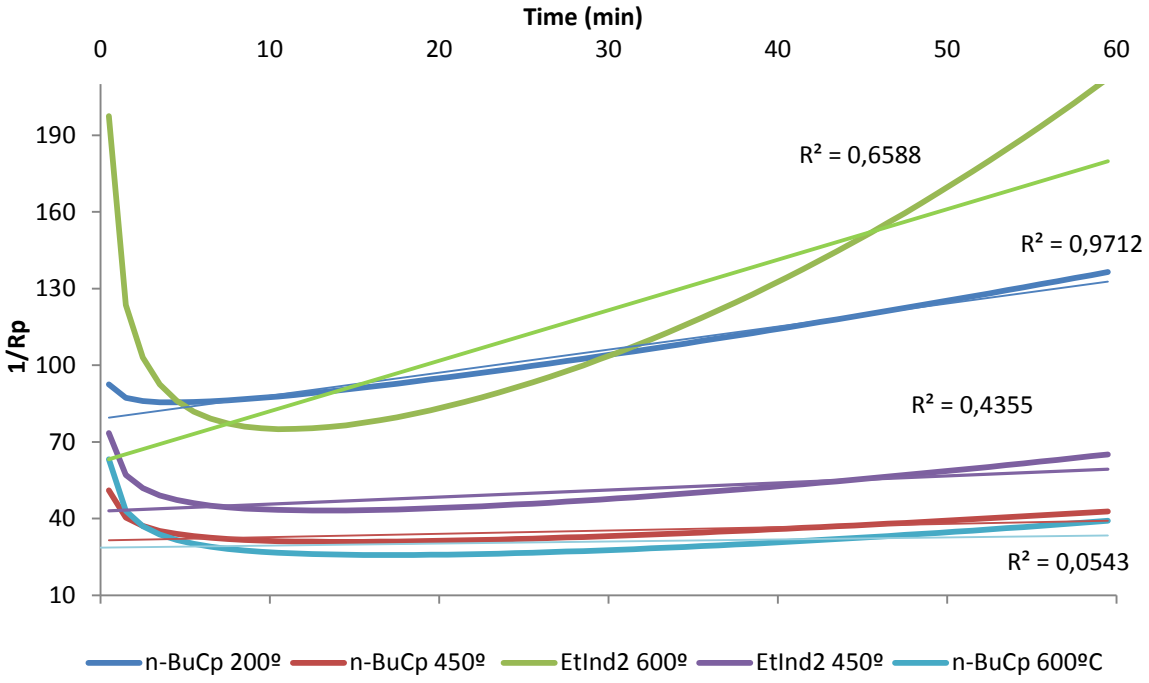

Figure 25 – Results of experimental data linearized and respective correlation line giving by noninstantaneous 1º order decay model

The experimental data obtained for the different catalysts studied was fitted to these linear equations. Figures 24 and 25 show respectively the experimental values of Ln Rp and 1/Rp versus time and the derived equations from linear regression, obtained in excel. As it may be seen from these plots and from the rather low values for R^2 these models do not fit well to the experimental data. This means that activation step is not instantaneous for none of the catalysts.

However, it´s possible to see that the one which is more close to linearity is n-BuCp 200ºC, with R-Square of 0,98 for instantaneous1º order decay and R-Square of 0,9712 for instantaneous 2º order decay.

In this case the Rp profiles were not plotted since from the previous fitting we concluded instantaneous model is not appropriate to explain the kinetics of this polymerization reaction

3.3 Non instantaneous model results

To be easier to fit the experimental data to the model and find a solution that converge, it was necessary to understand how does kinetic constants ka, kd, and kp, effect the polymerization rate. For that, was made a sensitivity analysis to study how the reaction rate was effected by changing the kinetic constants values.

Sensitivity analysis

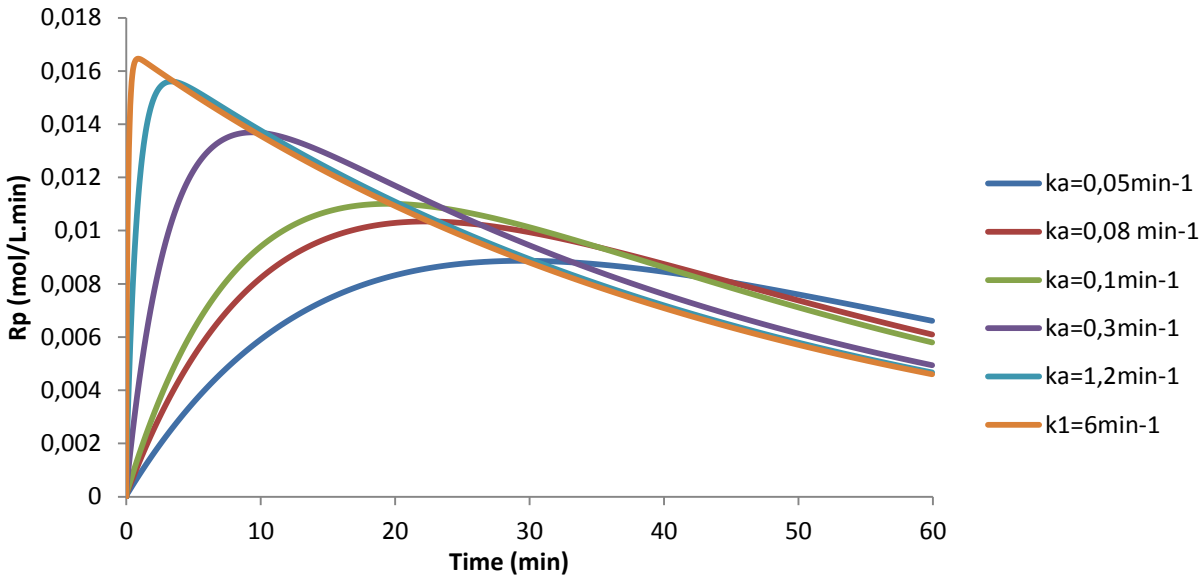

Figure 26 – Reaction rate for different ka values keeping other parameters fixed

It could be noticed that if we change ka for bigger values, the peak of maximum activity is higher and approximates to initial times of reaction. The limit of this situation is the instantaneous case where ka tends to infinite, giving a linear curve. Very high values of activity are also followed by some deactivation.

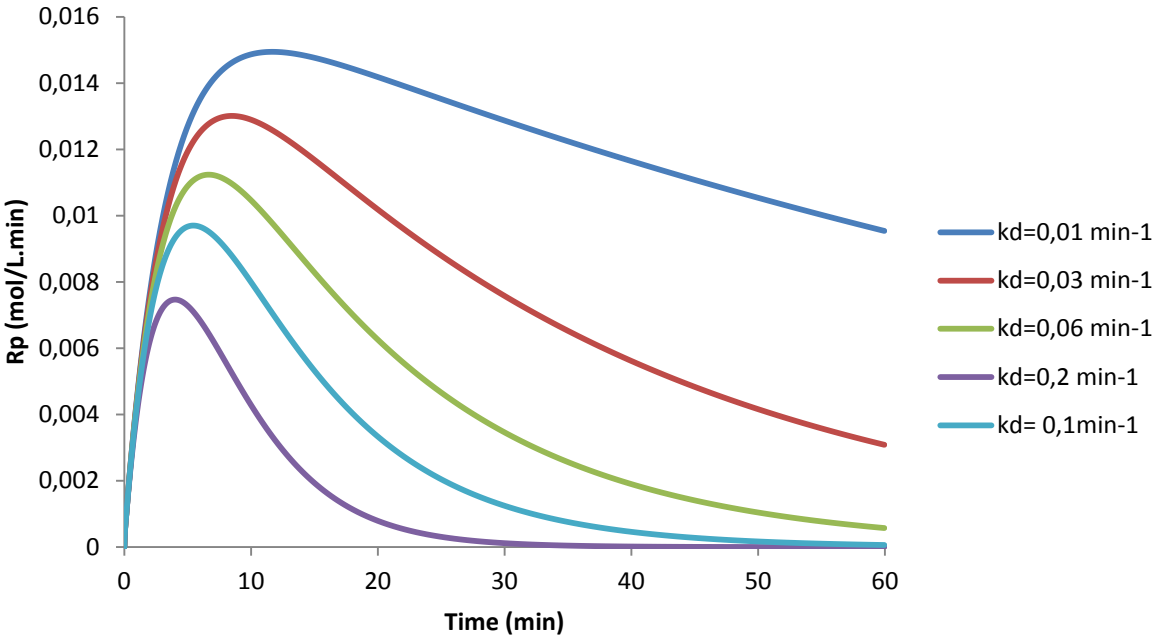

Figure 27 – Reaction rate for different kd values keeping other parameters fixed

In Figure 27, the effect of k_d on the reaction rate is shown. An increase of the constant deactivation value, leads to a faster decrease of R_p which is reflected in the slope of the curve after the peak.
The k_d constant is directly related with the intrinsic deactivation of the catalyst and it depends on catalyst nature. However it´s deactivation during reaction may also be affected by other parameters like the presence of impurities that linked to the catalyst. These impurities, in the present case, may came from the ethylene feed, which is not 100% pure and accumulates on reaction once we are in batch conditions. It can also come from the solvent. The reactor cleaning and the possible traces of oxygen and water at the beginning of reaction, may also affect the initial activity of the catalyst, affecting the maximum activity peak.

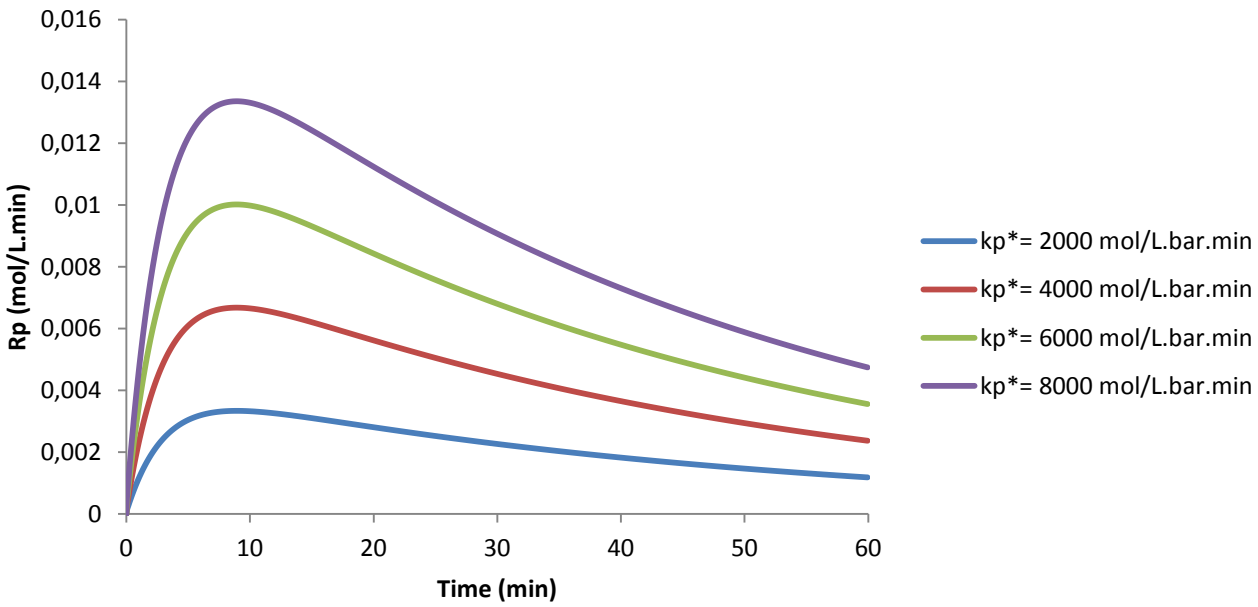

Figure 28 – Reaction rate for different kp* values keep other parameters fixed other

In what concerns the apparent propagation constant, kp*, it simply up or lower the reaction rate profile with consequent increase or decrease of the Rp values. This parameter gives the propagation rate of monomer insertion and depends on reaction conditions like pressure and temperature.

Results of noninstantaneous models

To obtain the kinetic constants of the model, the results of the sensitivity analysis above were used to make a first approximation fit by eye and choose the initial values for the constants to be used next in the fitting. Then, the mathematical fitting of experimental data to the model, was done by running the solver and minimizing the sum of quadratic deviations between the experimental and the calculated values. This procedure is just to facilitate the solution to converge once the nonlinearity gives a lot of solutions.

To have a better constant comparison, for each catalyst type were choose the two best experiments, ie, the two experiments that had overlap of the activities curves. The experiments samples choose are shown in table 2. All experiments conditions performed, can be consulted in appendix 2 board.

Table 2 – Samples choose for each catalyst type for kinetic modelling

Catalyst type	Sample
$(EtInd)_2ZrCl_2$ 450ºC	ANA_26; ANA_42
$(EtInd)_2ZrCl_2$ 600ºC	ANA_24; ANA_43
$(n\text{-}BuCp)_2ZrCl_2$ 200ºC	ANA_34; ANA_32
$(n\text{-}BuCp)_2ZrCl_2$ 450ºC	ANA_27; ANA_30
$(n\text{-}BuCp)_2ZrCl_2$ 600ºC	ANA_46

For $(n\text{-}BuCp)_2ZrCl_2$ 600ºC, it was not possible to obtain two overlapping activity curves, because the reproducibility was more difficult, probably due to some temperature increase during reaction.
To select and compare which model is better (1st or 2nd order decay) it was used the minimum square sum criteria given by solver run.

n-$BuCp_2$ 200ºC

Table 3 – Sum of square minimums for noninstantaneuos activation and 1st or 2nd order deactivation models

Sample	Model	$\sum \Delta^2$
ANA_34	**1st order**	**$2{,}56 \times 10^{-5}$**
ANA_34	**2nd order**	$4{,}52 \times 10^{-5}$
ANA_32	**1st order**	**$1{,}79 \times 10^{-5}$**
ANA_32	**2nd order**	$6{,}92 \times 10^{-6}$

Despite the 2nd order model fits better the ANA_32 experiment, the 1st order was chosen because the 2nd order behavior is just due to some problems in the fit of experimental data to the logistic equation.

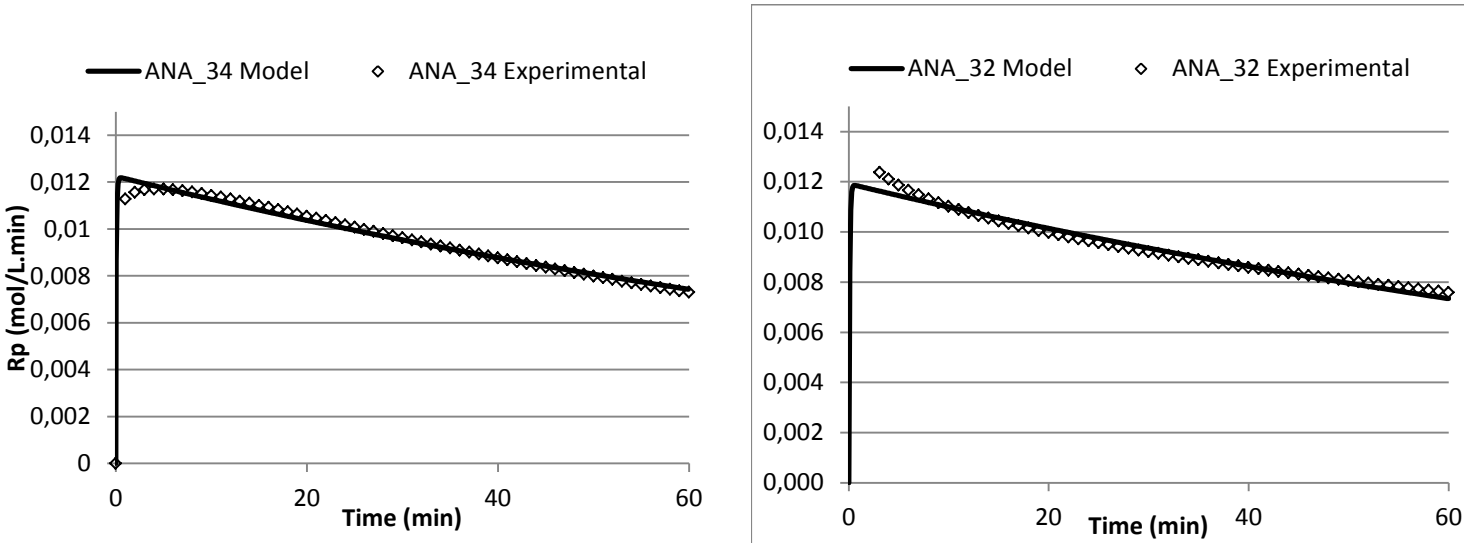

Figure 29 - Polymerization rate for n-BuCp 200ºC (ANA_34 and ANA_32 samples): experimental data and noninstantaneous activation 1st order deactivation model fitting.

Table 4 - Calculated kinetic parameters.

ANA_34	
Parameters	**Value**
Ka	12,3
Kd	8,34 x 10^{-3}
kp*	2,22 x 10^{4}
Pm	8,2
ε	0,1
[C0]	6,27 x 10^{-7}

ANA_32	
Parameters	**Value**
Ka	12,3
Kd	9,69 x 10^{-3}
kp*	2,26 x 10^{4}
Pm	8,5
E	0,1
[C0]	5,79 x 10^{-7}

n-BuCp$_2$ 450ºC

Table 5 – Sum of square minimums for noninstantaneuos activation and 1st or 2nd order deactivation models for n-BuCp 450ºC

Sample	model	$\sum \Delta^2$
ANA_27	**1st order**	**1,51 x 10^{-3}**
ANA_27	2nd order	1,63 x 10^{-3}
ANA_30	**1st order**	**2,05 x 10^{-3}**
ANA_30	2nd order	2,17 x 10^{-3}

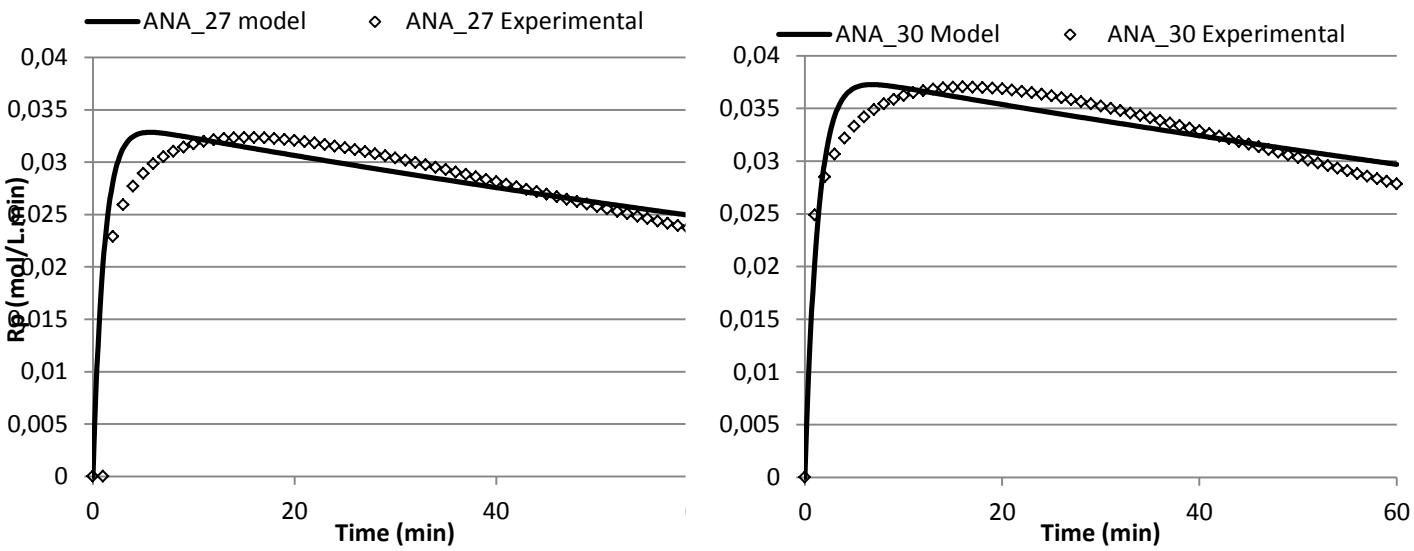

Figure 30 – Polymerization rate for BuCp 450ºC (ANA_27 and ANA_30 samples): experimental data and noninstantaneous activation 1st order deactivation model fitting.

Table 6 - Calculated kinetic parameters

ANA_27	
Parameters	**Value**
Ka	9,15 x 10^{-1}
Kd	5,27 x 10^{-3}
kp*	2,44 x 10^{4}
Pm	8,0
ε	0,1
[C0]	1,64 x 10^{-6}

ANA_30	
Parameters	**Value**
Ka	7,64 x 10^{-1}
Kd	5,25 x 10^{-3}
kp*	1,68 x 10^{4}
Pm	8,1
E	0,1
[C0]	2,82 x 10^{-6}

n-$BuCp_2$ 600ºC

Table 7 – Sum of square minimums for noninstantaneuos activation and 1st or 2nd order deactivation models for n-BuCp 600ºC

Sample	model	$\sum \Delta^2$
ANA_46	**1st order**	**2,11E-03**
ANA_46	2nd order	2,42E-03

In 600ºC case, looking for minimum-square, 1ºorder fits also better than 2ºorder.

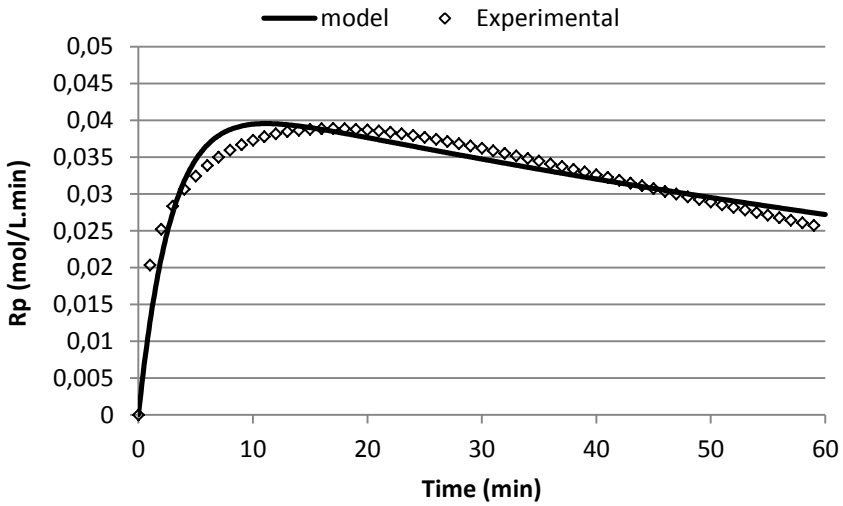

Parameters	Vue
Ka	3,44 x 10^{-1}
Kd	8,15 x 10^{-3}
kp*	1,98 x 10^{4}
Pm	8,0
ε	0,1
[Co]	2,72 x 10^{-6}

Figure 31 – Polymerization rate for BuCp 600ºC (ANA_46): experimental data and noninstantaneous activation 1st order deactivation model fitting. Calculated kinetic parameters.

Table 8 - Table resume of kinetic parameters for $(n\text{-BuCp})_2ZrCl_2$ 200ºC, 450ºC and 600ºC catalysts

Parameters	n-BuCp 200ºC (ANA_34)	n-BuCp 200ºC (ANA_32)	n-BuCp 450ºC (ANA_27)	n-BuCp 450ºC (ANA_30)	n-BuCp 600ºC (ANA_46)
Ka	12,3	12,3	$9{,}15 \times 10^{-1}$	$7{,}64 \times 10^{-1}$	$3{,}44 \times 10^{-1}$
Kd	$8{,}34 \times 10^{-3}$	$9{,}69 \times 10^{-3}$	$5{,}27 \times 10^{-3}$	$5{,}25 \times 10^{-3}$	$8{,}15 \times 10^{-3}$
kp*	$2{,}22 \times 10^{4}$	$2{,}26 \times 10^{4}$	$2{,}44 \times 10^{4}$	$1{,}68 \times 10^{4}$	$1{,}98 \times 10^{4}$
Pm	8,2	8,5	8,0	8,1	8,0
ε	0,1	0,1	0,1	0,1	0,1
[C0]	$6{,}27 \times 10^{-7}$	$5{,}79 \times 10^{-7}$	$1{,}64 \times 10^{-6}$	$2{,}82 \times 10^{-6}$	$2{,}72 \times 10^{-6}$

When comparing the kinetic parameters obtained from experiments performed in the same conditions it is possible to notice that the values of ka, kd and kp* are similar having the same order of magnitude.

In what concerns ka values, it is possible to see that n-BuCp 200ºC presents the higher ka value of 12.3 min-1. This is in accordance to the fact that the maximum of activity was attained in 1 minute of reaction The smaller activation constant, ka=0,344 min^{-1} was obtained for 600ºC. In this case it takes 11 minutes of reaction to attain the maximum of activity, For 450ºC the maximum activity was observed for 6 minutes and ka value is around 0,8 min^{-1}.(average of two experiments)

Regarding de deactivation, given by kd value, the higher value was for n-BuCp 200ºC and the lower one for n-BuCp 600ºC. Meaning that silica dehydroxydation at 600ºC followed by subsequent gives more stability in terms of activity than 200ºC in n-BuCp case.

Concerning kp apparent value, we can observed that the values are close with just a few deviation, with values around $2{,}2 \times 10^4$ $L.mol^{-1}bar^{-1}$, which means that in all experiments were used similar conditions of pressure and temperature.

$EtInd_2$ 450ºC

The Sum of square minimum deviations for noninstantaneuos activation and 1st or 2nd order deactivation models for supported EtInd2 catalyst is shown in Table 9.

Table 9 - Sum of square minimums for noninstantaneuos activation and 1st or 2nd order deactivation for EtInd2 450ºC

Sample	Model	$\sum \Delta^2$
ANA_26	**1st order**	**6,70 x 10^{-4}**
ANA_26	2nd order	8,99 x 10^{-4}
ANA_42	**1st order**	**9,10 x 10^{-4}**
ANA_42	2nd order	1,10 x 10^{-3}

For both experiments, we conclude again that the 1st order fits better.

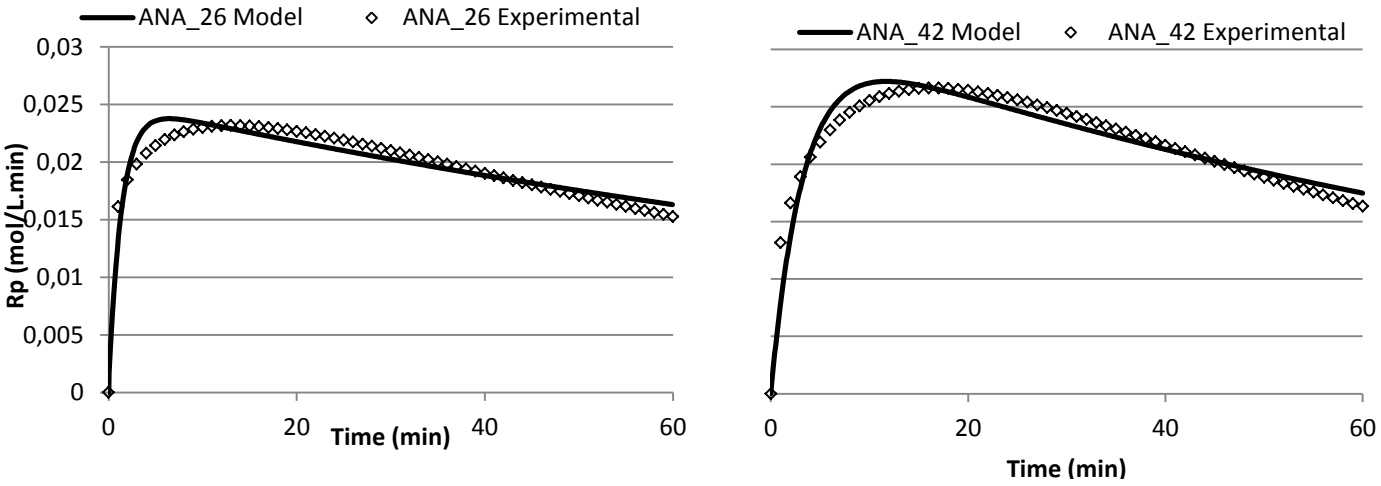

Figure 32 – Polymerization rate for $EtInd_2$ 450ºC (ANA_26): experimental data and noninstantaneous activation 1st order deactivation model fitting. Calculated kinetic parameters.

Table 10 - Calculated kinetic parameters

ANA_26	
Parameters	**Value**
Ka	7,16 x 10^{-1}
Kd	7,23 x 10^{-3}
kp*	1,56 x 10^{4}
Pm	8,4
ε	0,1
[C0]	1,89 x 10^{-6}

ANA_42	
Parameters	**Value**
Ka	3,0 x 10^{-1}
Kd	1,2 x 10^{-2}
kp*	1,67 x 10^{4}
Pm	8
ε	0,1
[C0]	2,28 x 10^{-6}

EtInd$_2$ 600ºC

Table 11 - Sum of square minimums for noninstantaneuos activation and 1st or 2nd order deactivation models for EtInd$_2$ 600ºC

Sample	model	R2
ANA_24	**1st order**	**1,50 x 10^{-4}**
ANA_24	2nd order	2,96 x 10^{-4}
ANA_43	**1st order**	**3,12 x 10^{-4}**
ANA_43	2nd order	4,52 x 10^{-4}

As the previous the 1st order fits better and with the same magnitude order.

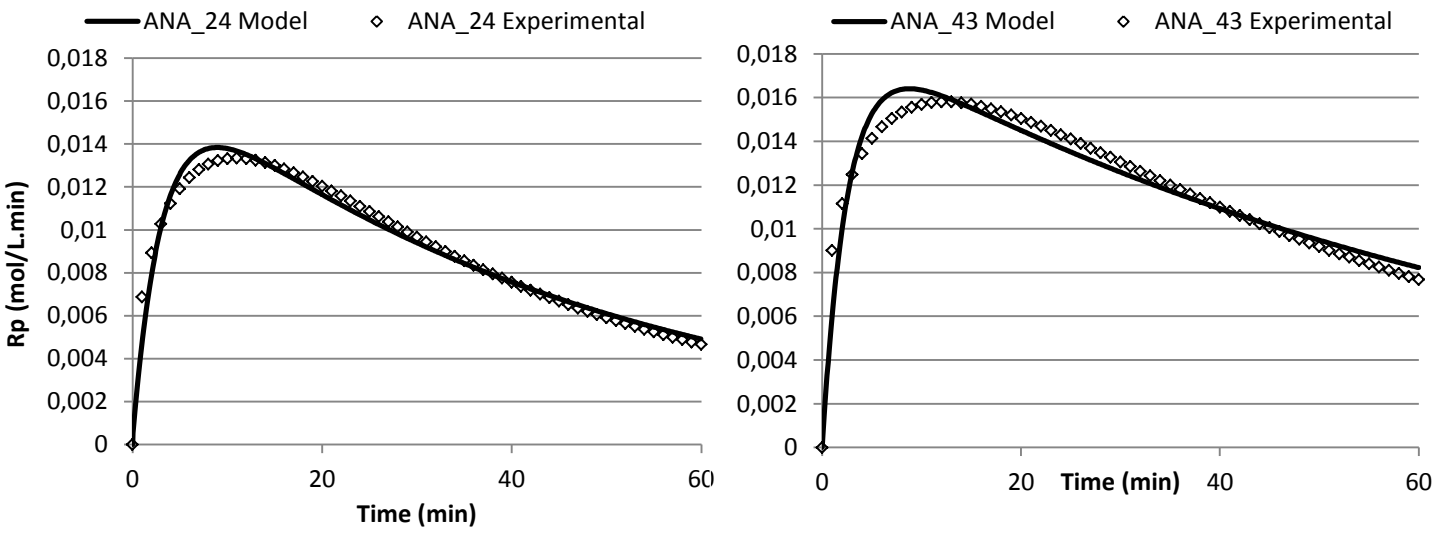

Figure 33 – Polymerization rate for EnInd$_2$ 600ºC (ANA_24 and ANA_43 samples): experimental data and noninstantaneous activation 1st order deactivation model fitting.

Table 12 - Calculated kinetic parameters.

ANA_24	
Parameters	**Value**
Ka	3,2 x 10^{-1}
Kd	2,16 x 10^{-2}
kp*	8,29 x 10^{3}
Pm	8,2
ε	0,1
[C0]	2,47 x 10^{-6}

ANA_43	
Parameters	**Value**
Ka	3,9 x 10^{-1}
Kd	1,7 x 10^{-2}
kp*	8,61 x 10^{3}
Pm	8
ε	0,1
[C0]	2,7 x 10^{-6}

Table 13 - Table resume of kinetic parameters for $EtInd_2ZrCl_2$ 450ºC and 600ºC catalysts

Parameters	$EtInd_2$ 450ºC (ANA_26)	$EnInd_2$ 450ºC (ANA_42)	$EnInd_2$ 600ºC (ANA_24)	$EnInd_2$ 600ºC (ANA_43)
ka	$7{,}16 \times 10^{-1}$	$3{,}0 \times 10^{-1}$	$3{,}2 \times 10^{-1}$	$3{,}9 \times 10^{-1}$
kd	$7{,}23 \times 10^{-3}$	$1{,}2 \times 10^{-2}$	$2{,}16 \times 10^{-2}$	$1{,}7 \times 10^{-2}$
kp*	$1{,}56 \times 10^{4}$	$1{,}67 \times 10^{4}$	$8{,}29 \times 10^{3}$	$8{,}61 \times 10^{3}$
Pm	8,4	8	8,2	8
ε	0,1	0,1	0,1	0,1
[C0]	$1{,}89 \times 10^{-6}$	$2{,}28 \times 10^{-6}$	$2{,}47 \times 10^{-6}$	$2{,}7 \times 10^{-6}$

Between the same experiments for 450ºC, we can see that there are some differences in ka and kd value. The smaller differences can be due to difficulty to get exactly the same reactor conditions in each batch, one condition was the ethylene pressure (Pm) as others.

For 600ºC the kp* is one order of magnitude less than 450ºC, meaning that the rate of monomer insertion in 600ºC case is the smallest one.

Table 14, shows the kinetic parameters given by the average values of experiments obtained in the same conditions.

Table 14 - Table resume with average of kinetic parameters for each catalyst type

	n-BuCp 200ºC	n-BuCp 450ºC	n-BuCp 600ºC	EtInd2 450ºC	EtInd2 600ºC
ka	12,3	0,8395	0,344	0,509	0,34
kd	$9{,}06 \times 10^{-3}$	$5{,}26 \times 10^{-3}$	$8{,}15 \times 10^{-3}$	1×10^{-2}	$1{,}93 \times 10^{-2}$
kp	$2{,}24 \times 10^{4}$	$2{,}0 \times 10^{4}$	$1{,}98 \times 10^{4}$	$1{,}61 \times 10^{4}$	$8{,}49 \times 10^{3}$

Looking to table resume, we could conclude that the deactivation is much high for $EtInd_2$ than for n-$BuCp_2$.

Ka values don´t differ too much, and concerning kp*, in general for $EtInd_2$ the propagation rate is less than n-$BuCp_2$.

3.4 MWD results

The following graphics show the MWD obtained directly from SEC analysis for each series of catalyst. The corresponding molecular parameters are presented on tables 15 and 16.

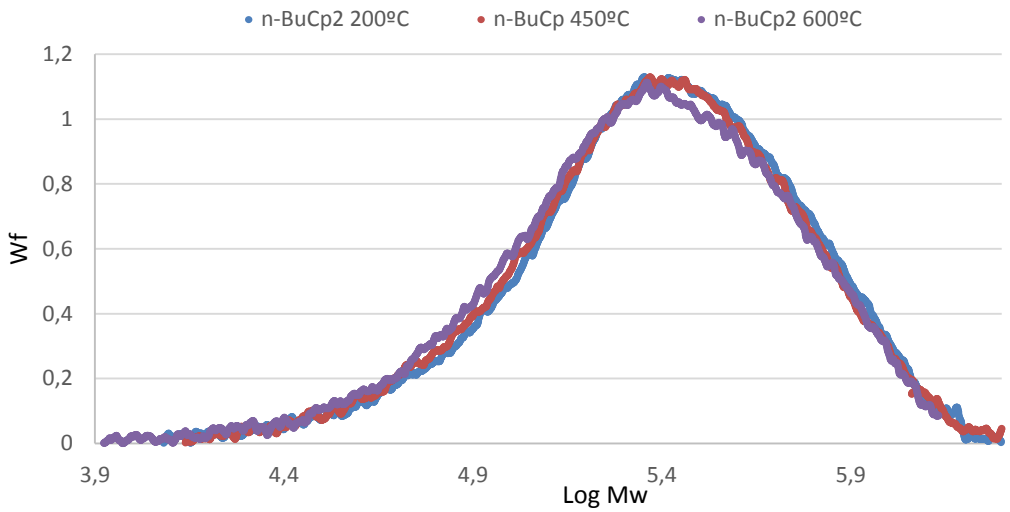

Figure 34 - Mass weight distribution for n-BuCp series

Table 15 - Mw, Mn and polydispersivity index of n-BuCp series

	n-BuCp 200ºC	n-BuCp 450ºC	n-BuCp 600ºC
Mn	167156	161822	148267
Mw	363369	336309	321794
PDI	2,17	2,08	2,17

Data from figure 38 for n-BuCp series shows very similar mass weight distributions with PDI around 2. Meaning that for this catalyst type independently of the dehydroxylation temperature used the MWD is very narrow and indicates that is a single site catalyst.

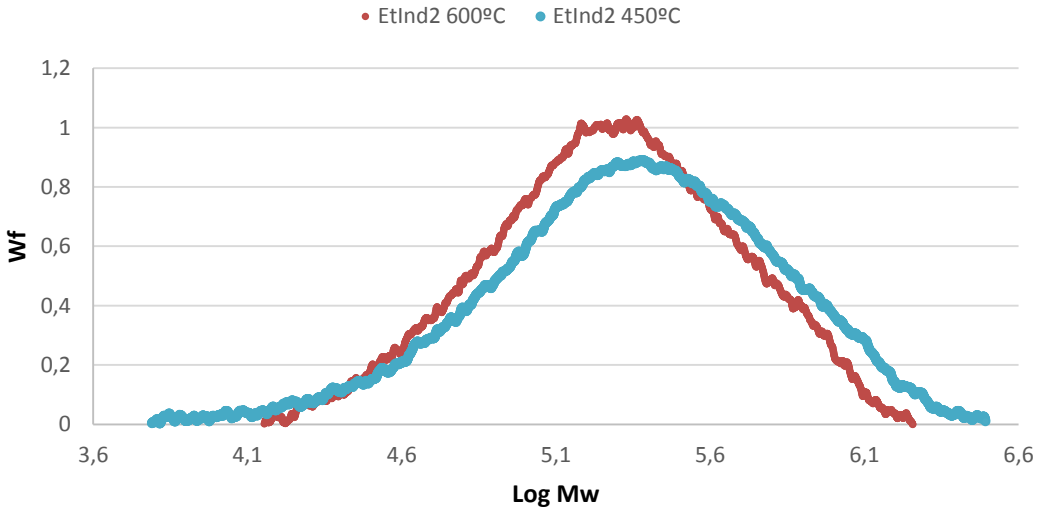

Figure 35 - mass weight distribution for EtInd2 series

Table 16 - Mw, Mn and polydispersivity index of n-BuCp series

	EtInd2 450ºC	EtInd2 600ºC
Sample	**ANA_26**	**ANA_24**
Mn	121211	125815
Mw	378376	280086
PDI	3,12	2,23

On the other hand, looking to EtInd2 series, it may be seen that dehydroxylation at 450ºC leads to a broader MWD with a PDI of 3,12. Meaning that in these conditions, the catalyst exhibits different surface features.

In terms of morphology, it was seen a very thin sticky powder not desirable for industry. To be a good polymer, it should look like spherical powder without sticking the reactor. To test if this could be caused by the use of TiBA it was done an experiment with TEA, and a better morphology was actually obtained.

3.5 Deconvolution results

The mathematical description of the model used in deconvolution is shown in appendix 3. To identify a representative number of families, the Flory´s distributions were adjusted to SEC analysis data by minimizing the objective function given by equation 4.9 and using the solver tool from excel.

$$x^2 = f \times \sum_{i=1}^{n\,SEC}\left(w_{Log\,Mw,i}{}^{SEC} - \sum_{j=1}^{x} mj\; w_{Log\,Mw,ji}{}^{model}\right)^2 + (1-f) \times (\Delta M_n^2 + \Delta M_w^2) \qquad (4.9)$$

$$\Delta M_n = M_{n\,SEC} - M_{n\,model} \qquad (4.9.1)$$

Where $w_{Log\,Mw,ji}$ is given by equation 1.6

x^2 minimizes not only the weight fractions ($w_{Log\,Mw}$) but also the deviation between Mn and Mw obtained by SEC analysis (experimental) and by the model, given respectively by equations 1.1, 1.2, 1.8 and 1.9 described on "Polymer microstructural characterization" subchapter. f, is a factor between 0 and 1, that decides the contribution of each parcel in the objective function. Several values were tested and it was assumed a value of 0,7 that give the lower x^2 values.

The minimization of the objective function leads to the estimation of m_x and $\hat{\tau}_x$ depending on the number of families considered.

The strategy adopted starts with two types of family sites and gradually progress to more until the minimized value of objective function value x^2 being achieved. When additional number of site types does not decrease the value of x^2 significantly, the best option is the lower number.[8]

The deconvolution was made only for $EtInd_2$ series, for a short (5 or 15 min) and a long period time (1 hour). Although other attempts were made i. e. 30 min, these experiments should be repeated because samples revealed SEC results with a lot of noise.

The results obtained with SEC are in table 17.

Table 17 – table resume of MWD SEC experimental results

	EtInd2 600ºC	EtInd2 600ºC	EtInd2 450	EtInd2 450
Sample	ANA_20	ANA_24	ANA_1	ANA_26
Reaction time (min)	5	60	15	60
Mn	122026	123859	53400	121211
Mw	259574	293728	156609	378376
PDI	2,1	2,4	2,9	3,1

0

0

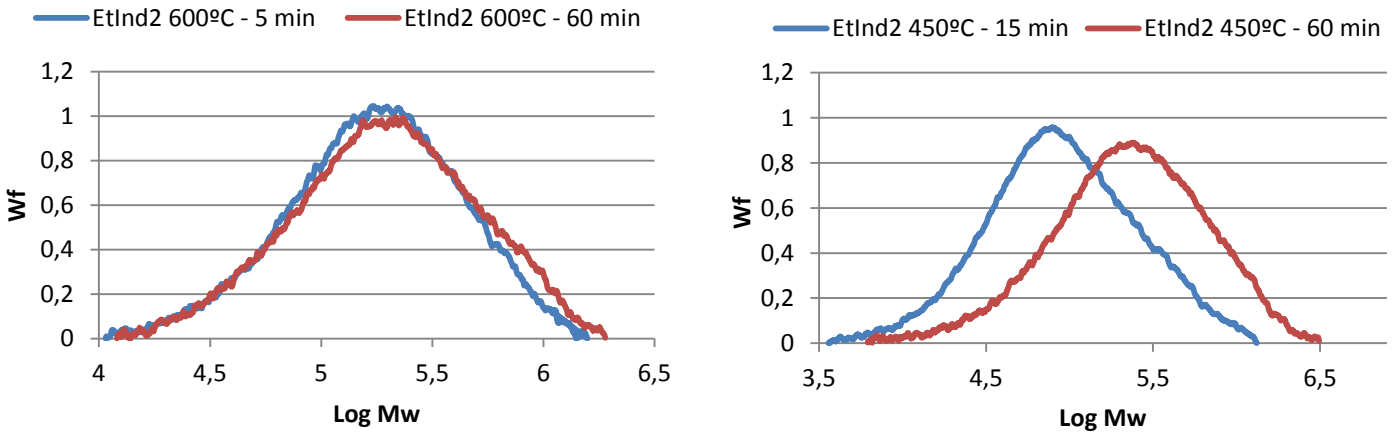

Figure 36 – SEC experimental molecular weight distributions with EtInd2 450ºC and 600ºC for a short and long reaction times

With EtInd2 600ºC catalyst between 5 to 60 min it can be seen that the overall experimental molecular weights doesn't change too much. Mn change only 122026 to 123859 g/mol and Mw 259574 to 293728 g/mol

However with EtInd2 450ºC the molecular weights increase with time reaction. Mn increases highly 53400 to 121211 g/mol and Mw 156609 to 378376 g/mol

Using the fitting procedure previously described, we conclude by x^2, in table 18, that for $EtInd_2$ 600ºC and 5 minutes the best fit is two families since x^2 value only decrease 0,2% between 2 to 3 family sites. For 1 hour of reaction the best fit is three families.

Table 18 - MWD deconvolution parameters of 2 and 3 different site types

		Tr= 5 minutes (ANA_20)				Tr=60 minutes (ANA_24)			
nºsites		1	2	3	All	1	2	3	All
2	M	0,590	0,410			0,593	0,407		
	Mn	75051	193218,2		100168,4	77990	240265,9		107577,9
	Mw	147667,9	385502,8		245183,2	155980,7	480531,7		288143,3
	x^2	**0,4238**				0,894			
3	M	0,588	0,409	0,0028		0,584	0,386475	0,030	
	Mn	75151	193359,4	64023	100172	81989	245621,3	37584	105400,4
	Mw	147667,9	385502,8	128046,9	244977,8	163977,9	491242,5	75168	287800,4
	x^2	0,4229				**0,805**			

In Figure 38 it is depicted the contribution of each family of active sites (characterized by a given average molar mass and PDI) to the overall MWD. Moreover it is seen that the curve predicted by the model (red) and the experimental (blue) one are in close agreement.

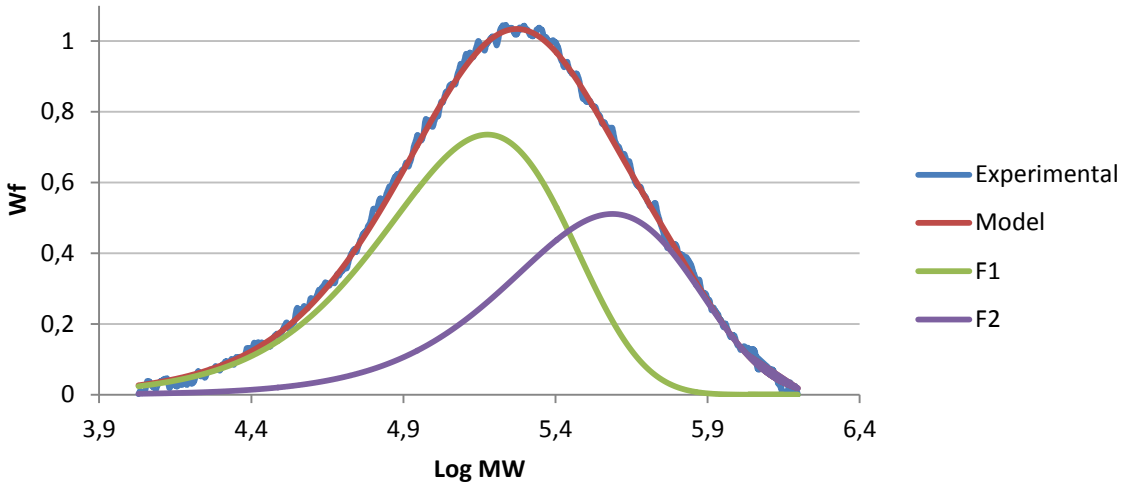

Figure 37 - MWD of families for EtInd2 600ºC 5 min

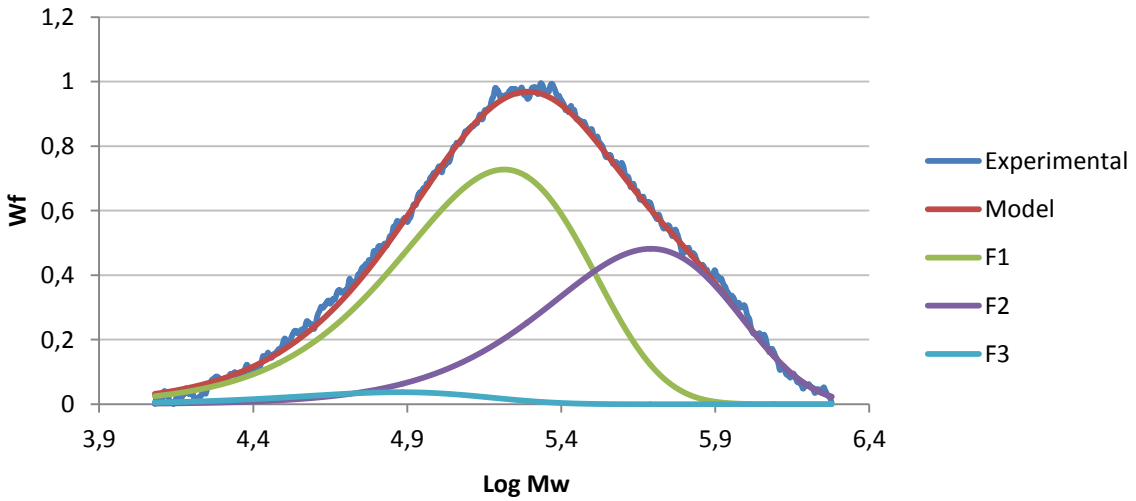

Figure 38 - MWD of families for EtInd2 600ºC 60 min (ANA_24)

Comparing Figures 40 and 41, it is possible to notice that family one (F1) and family two (F2) maintained the same peak intensity. The main difference is the appearance of a third family after 60 minutes of reaction.

A possible interpretation for this behavior is that at the beginning of the reaction there are two types of active sites with different polymerization rates. One corresponding to the major contribution that produces

the polymer chains with lower molar masses and the other that produces the higher molar masses. However after 60 minutes of reaction, a third site type appears although in a very small contribution.

EtInd2 450ºC

Since for this case a broader MWD was noticed, the fitting families were extend to four. It can be concluded in table 12 through x^2 value, that the best fit is obtained for three families for both times.

Table 19 - MWD deconvolution parameters of 2, 3 and 4 different site types

		Tr=15 minutes (ANA_1)					Tr= 60 minutes (ANA_26)				
nºsites		1	2	3	4	All	1	2	3	4	All
2	m	0,360	0,640				0,544	0,456			
	Mn	132657	35158			47800	84296	293022			124899
	Mw	265315	70316			140484	168592	586044			359106
	x^2	1,005					1,64				
3	m	0,276	0,576	0,148			0,509	0,357	0,134		
	Mn	92438	33336	191370		47537	110592	332575	45826		116275
	Mw	184876	66672	382740		146072	221185	665150	91652		362302
	x^2	**0,558**					**0,314**				
4	m	0,249	0,467	0,184	0,099		0,479	0,366	0,124	0,031	
	Mn	85094	33922	177022	29717	56356	106205	327322	58572	11007	129185
	Mw	170188	67844	354045	59433	139350	212410	654645	117144	22013	355857
	x^2	0,569					0,657				

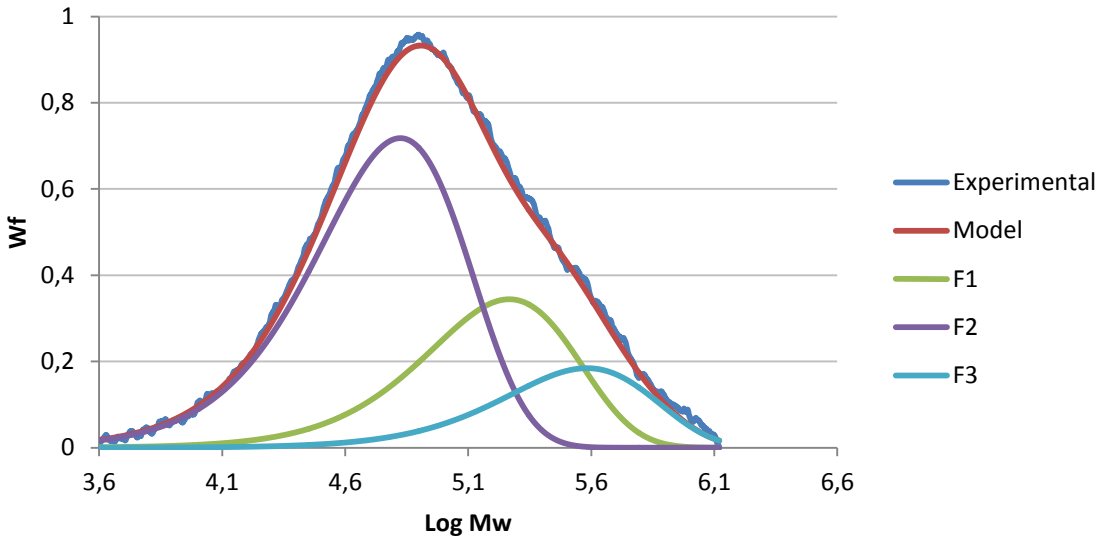

Figure 39 - MWD of families for EtInd2 450ºC 15 min (ANA_1)

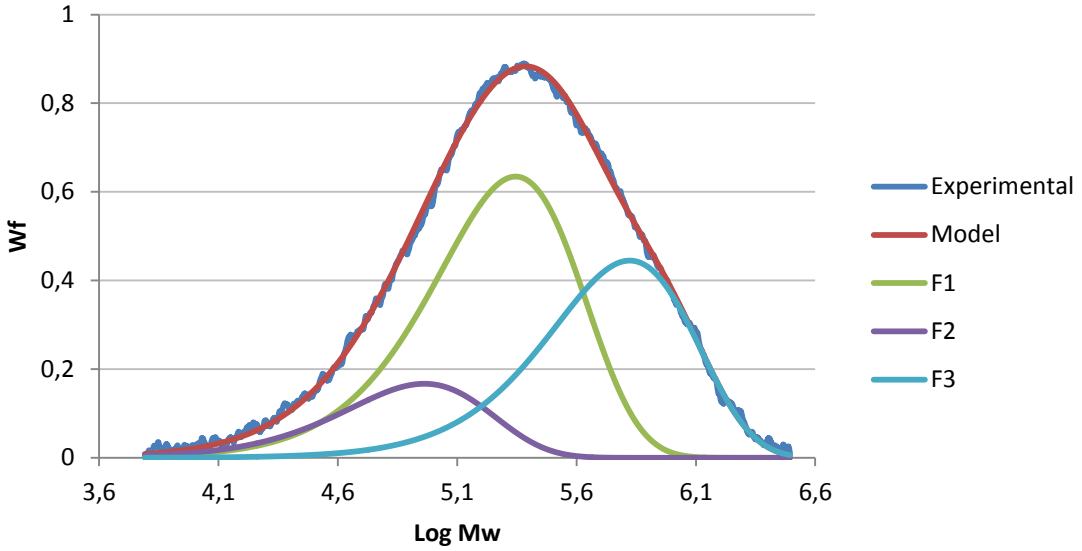

Figure 40 - MWD of families for EtInd2 450ºC 60 min (ANA_26)

From figures 39 and 40, it may be seen that between 15 and 60 minutes, the contribution of each family of active sites to the overall MWD is changing together with the average molar masses of each family. In all cases the Mn and Mw values increase from 5 to 60 minutes

So, initially the major contribution to overall MWD (m=0,58) is from the lower molar mass polymer (F2), with an average Mn around 33000, but after 60 min this lower molar mass family is centered around 45000 and its contribution decreased to only 0,13. This means that the proportion of this family of active sites is decreasing along time. On the contrary the contribution of the other two families centered

respectively at intermediate and higher molar masses increased considerably from 0,28 to 0,53 and from 0,15 to 0,36

We can say also as a possible interpretation that there are 3 families, each one with different reaction behavior during the reaction. For the first family (F1), at the beginning are produced chains with considerable contribution of small molar masses. Then after 60 minutes of reaction, the same family produces chains with the same molar mass but with less contribution, meaning that propagation rate of this family is decreasing. The opposite happens with other two families, the rates of those are increasing, and after 60 minutes the second family is the one with higher molar mass impact.

Nonlinear optimization problems are frequently subject to multiple solutions, but because Flory distribution has a fixed width (PDI= 2), the MWD deconvolution procedure is generally quite robust.

3.6 DSC results

The polymer samples obtained with the n-BuCp catalyst, were analyzed by DSC. Results are shown in Table 15.

Table 20 –Crystallinity and melting temperature of for polymer n-BuCp samples

n-BuCp series				**EtInd2 series**		
Temperature	**Sample**	**Crystallinity (%)**	**T_M (ºC)**	**Sample**	**Crystallinity (%)**	**T_M (ºC)**
200ºC	ANA_34	57,93	137,67	-		
	ANA_32	57,84	136,83	-		
450ºC	ANA_27	61,43	135	ANA_26	65,72	138,33
	ANA_30	61,41	136,33	-		
600ºC	ANA_35	61,7	137,83	ANA_24	64,36	134,33
	ANA_44	61,78	135,67	-		

It may be seen that the polymerizations made in the same conditions lead to polymer samples with very close values for crystallinity

Moreover the crystallinity and Tm values of the samples obtained with $EtInd_2$ catalyst are slightly higher than those for n-BuCpcatalyst,. In n-BuCp series the lower crystallinity is observed for the 200ºC sample and the other two samples, at 450ºC and 600ºC, present very similar values.

The crystallinity of the samples versus polymerization time for EtInd2, 450ºC and 600ºC, is shown respectively in figures 44 and 45

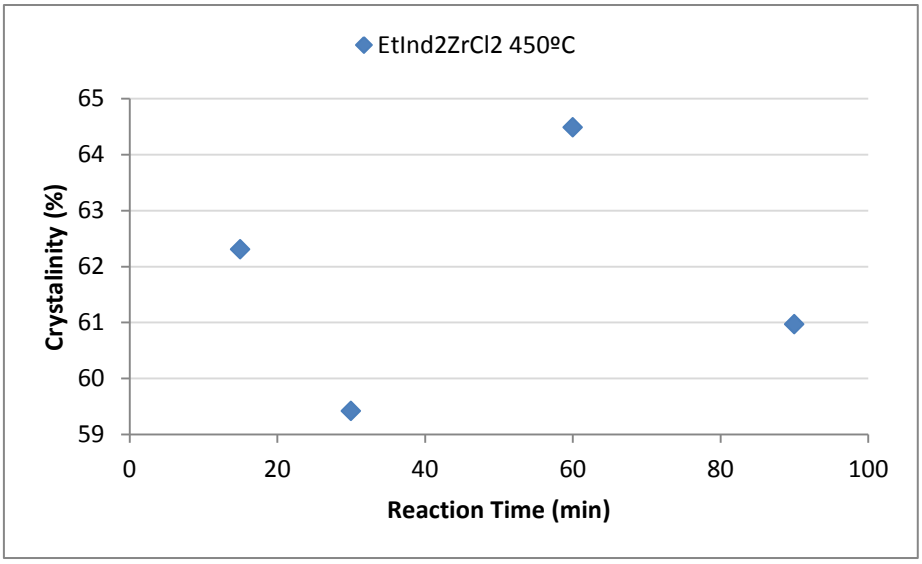

Figure 41 – Crystallinity for different time reactions

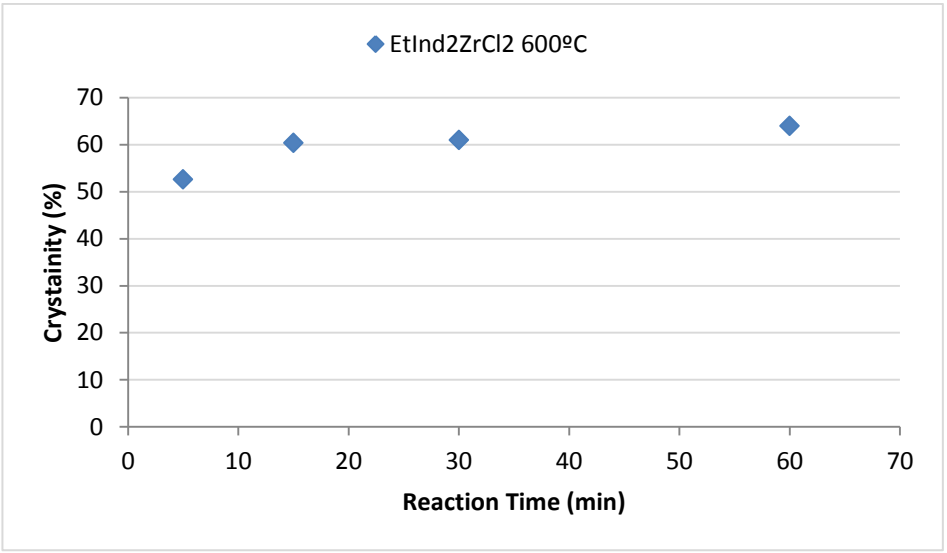

Figure 42 – Crystallinity for different time reactions

Regarding EtInd2 600ºC it is noticed an increase of crystallinity with time. However, for 450ºC no relation between crystallinity and time is observed.

It will be necessary to repeat these experiments to be sure of how crystallinity is affected by reaction time.

Cap 4. Conclusions

Particular care had to be taken In this work, to make sure that the activity profile are representative of the experimental conditions used and reproducible. This demands using optimized and reproducible polymerization conditions from one batch to another. However the reproducibility is a difficult task to achieve in this work, due to the sensitivity of this type of catalysts to traces of water, oxygen or other polar compounds. This reflects in a difficult with experimental handling. Some of the difficulties will be mentioned below.

- It was difficult to have an accurate weight value inside the glovebox, because the renewing the atmosphere glove box with inlets of argon, causes fluctuations in the balance weights.
- Stirring rate was not constant, causing non homogenous zones that may affect the activity;
- Handling the controller ethylene valve in order keep the initial pressure exactly in the same value for each batch, was not always easy to achieve.
- It was difficult to detect the starting point because when the valve of ethylene feed is open it was noticed some pressure fluctuations inside the reactor.
- The heptane volume is not precise because is measured by eye.
- The exact fraction of active sites is also difficult to estimate depending on numerous factors like the time exposure or some oxygen inlet causing degradation with time.

Some of these factors can be improved with experience time or by changing reactor configuration.

Concerning the kinetic modelling, a general model for a single site catalysts was applied and several variations of this model, with differences on the activation and deactivation steps were analyzed. Results have shown, for both type of catalyst studied, that the best fit was obtained for the non-instantaneous activation and first order deactivation model. For each system the corresponding kinetic constants ka, kp and kd, were evaluated.

The most difficult catalyst to model was n-BuCp 600ºC with X^2 values of 10^{-3} magnitude order, compared with better values of the others with 10^{-4} – 10^{-5} magnitude order. It was also the only experiment that wasn´t possible to get reproducibility. This may be related with the fact that temperature raises around 3ºC during one hour of reaction. For the other experiments was noticed an increase only of 0,5-1ºC.

Despite this model being mostly used for homogeneous catalyst, it revealed to be also good for this heterogeneous catalysts since the model fitted quite well the experimental data.

Regarding MWD, since these two catalysts are single site and were well fit by single site model, it was expected a PDI of 2. However for EtInd2ZrCl2 450ºC we noticed same deviation from single site once the PDI value is around 3. In fact, it was observed a good morphology for n-BuCp with a spherical powder not sticky and on the other hand for EtInd2 the polymer was a very sticky powder.

This could be related with use of TiBA. TiBA act as a scavenger cleaning all the impurities remain in solvent, argon and ethylene compounds. The volume of TiBA added is the optimized volume for not affecting reaction rate (getting from some previous studies). However TiBA could also somehow

interferes with reaction affecting not only activity but also the polymer microstructure. To confirm that TiBA affects the microstructure was performed an experiment with TEA and was obtain similar powder to n-BuCp althought with less activity. Meaning that TEA could be a better choice than TiBA in future experiments.

Although we could get some conclusion from results, there are some factors that need to be considered. The way the polymer sample is dried is very important, because remains of any solvent are evaporated and interferes with crystallinity and melting point measures. Also the remains of catalyst, although are in less quantity than polymer, could have some interference. Considering these factors and also a DSC accuracy of ±5% on the crystallinity measurement, it is necessary to repeat again the same experiments to conclude precise results.

Cap 5. Future Perspectives

There is a lot of continuous investigation work still to be done in this area. This investigation studies will helps to improve catalyst performance and to develop new applications.

Some aspects must be taken into account in order to improve the work done in the scope of this thesis. An important issue is the reproducibility of the experiments, and to maintain exactly the same conditions is a first point to improve. Some of these aspects could be eliminated with reactor design modifications.

Another aspect to be taken into consideration is the impact of use TEA instead of TIBA once better microstructure morphology (less sticky and spherical powered) was noticed with $EtInd_2ZrCl_2$ with TEA although with less activity.

Another aspect is to complete the study for $EtInd_2$, including the 200ºC dehydroxydation temperature and determine definitely if for this catalyst the dependence of activity on dehyoxydation temperature follows a different pattern than the one exhibited by $n\text{-}BuCp_2$.

It could also be interesting to do experiments at different polymerization temperatures and determine the values for k_0 and Ea constants with Arrenius law. For each catalyst at a given dehydroxydation temperature. With these experiments we can also see how activity is affected by temperature change. Concluding if the reason why was difficult to get reproducibility in $n\text{-}BuCp_2$ 600ºC case may be related due to the increase of temperature observed during the polymerization..

Finally these new experiments will also enable to validate the model by changing reaction conditions like temperature and pressure and then determine if these new data is well fitted by the proposed model.

References

[1] CHAKRAVARTI, S.; RAY, W. Harmon (2001) Kinetic study of olefin polymerization with a supported metallocene catalyst. Ethylene/1-hexene copoymerization in gas phase, Wisconsin, Journal of Applied Polymer Science 80, 1096-1119

[2] Research in catalytic construction by California University: http://www.chemengr.ucsb.edu/~ceweb/faculty/scott/pdf/International%20Innovation.pdf date: 1/6/04)

[3] TISSE, Virginie F.; BOISSON, Christophe; MCKENNA, Timothy F.L. (2014) Activation and deactivation of the polymerization of ethylene over rac-EtInd2ZrCl2 and (n-BuCp)2ZrCl2 on na activating silica support, Macromol. Chem. Phys, DOI, 10.1002

[4] SANTOS, João H. Z.; FISCH, Adriano G. (2008) Alargamento da distribuição de massa molar de polimeros sintetizados com catalisadores metalocênicos dual-site, Quim. Nova Vol 31 No 5, 1199-1207

[5] Juraj kosek research group: http://www.kosekgroup.cz/index.php?option=com_content&view=article&id=49:mathematical-modeling-of-polymer-particle-growth-and-morphology-effective-scale-models&catid=29&Itemid=108, 1/9/04

[6] http://www.hindawi.com/journals/jic/2013/902192/sch2/

[7] BERGSTRA, Michiel F.; WEICKERT, Gunter (2005) Ethylene polymerization kinetics with heterogeneous metalocene catalyst – comparason of gas and slurry phases, Finland, Macromol. Mater. Eng. 290, 610-620

[8] MCKENNA, T.F.L; SOARES, J.B.P; (2012) Polyolefin Reaction Engineering, Germany: Wiley-VCH

[9] CHIN-SAN, (2008) Handbook Of Size Exclusion Chromatography And Related Technique, p. 488

[10] Hasan A.T.M. Kamrul, Multiplicity of active-sites in heterogeneous Ziegler-Natta catalyst and it´s correlation with polymer microstructure, Bangladesh J.Sci Ind. Res. 46 (6), 487-494, 2011

[11] BELELLI, Patricia G.; FERREIRA, Maria L.; DAMIANI, Daniel F. (2002) Silica-supported metallocene for ethylene polymerization, Argentina: Elsevier Science B.V, Applied catalysis A: general 228 189-202

[12] HAN, Joong Jin; LEE, Hyung Woo; YOON, Won Jung; CHOI, Kyu Yong, (2007), Rate and molecular weight distribution modeling of syndiospecific styrene polymerization over silica-supported metallocene catalyst, Korea, Elsevier Ltd, Polymer 48, 6519-6531

[13] ATIQULLAH, Muhammad; ANANTAWARASKUL, Siripon (2014) Silica-supported (n-BuCp)2ZrCl2: affect of catalyst active center distribution on ethylene-1-hexene copolymerization, Polym Int 63, 955-972

[14] BERGSTRA, Michiel F.; WEICKERT, Gunter (2006) Semi-batch reactor for kinetic measurements of catalyzed olefin co-polymerizations in gas and slurry phase, Chemical Engineering Science 61, 4909-4918

[15] GRIEKENM, R. Van; CARRERO, A.; PAREDES, B.; SUAREZ, I. (2007) Ethylene polymerization over supported MAO/ (n-BuCp)2ZrCl2 catayst: Influence of support properties, Spain, European Polymer Journal 43, 1267-1277

[16] BOCHMANN, Manfred (2004) Kinetic and mechanistic aspects of metallocene polymerization catalyst, UK, Journal of Organometallic Chemistry 689 3982-3998

[17] TIONI, Estevan; BROYER, Jean Pierre; MONTEIL, Vincent; MCKENNA, Timothy (2012) Influence of reaction conditions on catalyst behavior during the early stages of gas phase ethylene homo- and copolymerization, Netherlands, Ind. Eng. Chem. 51, 14673-14684

[18] MCAULEY, Kim B.; HSU, James C.C.; BACON, David W. (2005) Mathematical model and parameter estimation for gas-phase ethylene/hexene copolymerization with metallocene catalyst, Canada, Macromol. Mater. Eng 290, 537-557

[19] MOGILICHARLA, Anitha; MITRA Kishalay; MAJUMDAR, Saptarshi (2014) Modeling of propylene polymerization with long chain branching, India, Chemical Engineering Journal 246, 175-183

[20] MCAULEY, Kim B.; KOU, Bo (2005) Mathematical model and parameter estimation for gas-phase ethylene homopolymerization with supported metallocene catalyst, Canada, Ind.Eng. Chem. Res. 44 2428-2442

[21] MCKENNA, Timothy F.; SOARES, João B.P (2001) Single particle modelling for olefin polymerization on supported catalyst: A review and proposals for future developments, Canada, Chemical Engineering Science 56, 3931-3949

[22] CHU, Kyung-Jun; SOARES, João B. P.; PENLIDIS, Alexander (2000) Variation of molecular weight distribution (MWD) and short chain branching distributions (SCBD) of ethylene/1-hexene copolymers produced with diffrent in-situ supported metallocene catalysts, Canada, Macromol. Chem. Phys. 201, 340-348

[23] ABDEL-BARY, Elsayed M. (2003) handboock of plastic films, UK, Rapra tecnology limited, 44-45

[24] Website created by Dr. Kermit Duckett, Professor of Textile Science teaching course on "Nonwovens Science & Technology II":http://www.engr.utk.edu/mse/Textiles/Polymer%20Crystallinity.htm (1/11/04)

APPENDIX 1 – Runge-Kutta 4 order numerical equations

$y' = f(t, y(t))$, Where y (t) is the the propagation rate, Rp, in instant t.

$$y_{n+1} = y_n + \frac{h}{6}(k_1 + 2k_2 + 2k_3 + k_4)$$

$$h = t_{n+1} - t_n$$

$$k_1 = f(y_n, t_n)$$

$$k_2 = f(y_n + \frac{k_1}{2}, t_n + \frac{h}{2})$$
$$k_3 = f(y_n + \frac{k_2}{2}, t_n + \frac{h}{2})$$
$$k_4 = f(y_n + k_3,\ t_n + h)$$

In this case was considered a step value (h) of 0,1 and the following initial condition

$$y_0(t_0) = 0$$

These equations were implemented iteratively in excel.

APPENDIX 2 – Table with conditions of experiments performed

Sample Name	*Catalyst*	*Temp cat (ºC)*	*cat mass (mg)*	*Agitation (rpm)*	*Time react (min)*	*P Total (bar)*	*yield PE (g)*	[C0] (mol/L)	*Actvity avg (g/g.h)*
Homopolymerization in Slurry									
ANA_1	Et(Ind)2ZrCl2	**450**	15	300	**15**	10	3,1	1,18E-06	827
ANA_2	Et(Ind)2ZrCl2	**450**	16	300	**30**	10,4	2,2	1,26E-06	275
ANA_3	Et(Ind)2ZrCl2	**450**	17,4	300	**60**	10,6	26	1,37E-06	1494
ANA_4	Et(Ind)2ZrCl2	**600**	17,5	335	**15**	10,6	2	-	457
ANA_5	Et(Ind)2ZrCl2	**600**	18,8	337	**30**	10,8	0,5	-	53
ANA_6	Et(Ind)2ZrCl2	**600**	20,9	332	**60**	10,6	2,56	-	122
ANA_7	*n-BuCpZrCl2*	**450**	21	340	**120**	10,8	19,56	1,38E-06	466
ANA_8	Et(Ind)2ZrCl2	**450**	26,3	330	**60**	10,5	17,6	2,08E-06	669
ANA_9	Et(Ind)2ZrCl2	**200**	21,2	330	**60**	10,3	2,3	1,07E-06	108
ANA_10	Et(Ind)2ZrCl2	**450**	20	326	**30**	9	2,5	1,58E-06	250
ANA_11	Et(Ind)2ZrCl2	**450**	25	370	**90**	9,2	31,4	1,97E-06	837
ANA_12	Et(Ind)2ZrCl2	**600**	25,5	350	**60**	9,5	6,9	-	271
ANA_13	Et(Ind)2ZrCl2	**600**	25	337	**30**	9,3	2,4	-	192
ANA_14	*n-BuCpZrCl2*	**600**	24,6	340	**90**	9,2	16,4	2,48E-06	444
ANA_15	Et(Ind)2ZrCl2	**450**	25	338	**30**	9,3	3,2	1,97E-06	256
ANA_16	n-BuCpZrCl2	**200**	29	340	**45**	9,3	6,5	6,99E-07	299
ANA_17	Et(Ind)2ZrCl2	**600**	25	368	**80**	10,2	13,1	2,25E-06	393
ANA_18	Et(Ind)2ZrCl2	**600**	25	355	**60**	8,7	11,5	2,25E-06	460
ANA_19	Et(Ind)2ZrCl2	**600**	26,3	350	**30**	8,9	7,1	2,36E-06	540
ANA_20	Et(Ind)2ZrCl2	**600**	23,6	352	**5**	9,3	0,84	2,12E-06	427
ANA_21	Et(Ind)2ZrCl2	**600**	26	350	**60**	8,9	15,8	2,34E-06	608
ANA_22	Et(Ind)2ZrCl2	**600**	28	400	**90**	8,3	-	2,52E-06	-
ANA_23	Et(Ind)2ZrCl2	**600**	26	385	**53**	8,8	-	2,34E-06	
ANA_24	Et(Ind)2ZrCl2	**600**	27,5	369	**60**	9,2	8,4	2,47E-06	305
ANA_25	Et(Ind)2ZrCl2	**450**	29	350	**60**	9,1	30	2,29E-06	1034
ANA_26	Et(Ind)2ZrCl2	**450**	24	385	**60**	9,2	18,6	1,89E-06	775
ANA_27	n-BuCpZrCl2	**450**	25	376	**60**	9	24,7	1,64E-06	988
ANA_28	Et(Ind)2ZrCl2	**450**	23	350	**60**	8,8	17,2	1,82E-06	748
ANA_29	n-BuCpZrCl2	**600**	23	350	**60**	9,3	19,1	2,32E-06	830
ANA_30	n-BuCpZrCl2	**450**	28	374	**55**	9,1	29,5	2,82E-06	1149
ANA_31	Et(Ind)2ZrCl2	**450**	24	370	**30**	9,3	9,2	1,89E-06	767
ANA_32	n-BuCpZrCl2	**200**	24	373	**60**	9,2	9	5,79E-07	375
ANA_33	n-BuCpZrCl2	**450**	24	350	**60**	9	8,5	1,58E-06	354
ANA_34	n-BuCpZrCl2	**200**	26	356	**60**	9,2	9	6,27E-07	346
ANA_35	n-BuCpZrCl2	**600**	27	324	**60**	8,9	32,7	2,72E-06	1211
ANA_36	Et(Ind)2ZrCl2	**600**	26	350	**15**	9,4	8,1	2,34E-06	1246
ANA_37	Et(Ind)2ZrCl2	**450**	25	325	**15**	9,6	8,9	1,97E-06	1424
ANA_38	Et(Ind)2ZrCl2	**600**	26	324	**30**	8,9	5,3	2,34E-06	408
ANA_39	Et(Ind)2ZrCl2	**200**	25	330	**30**	9,3	2,2	$1,26x10^{-6}$	176
ANA_40	n-BuCpZrCl2	**600**	20	324	**50**	9	-	-	-
ANA_42	Et(Ind)2ZrCl2	**450**	28,9	-	**60**	9		$2,28x10^{-6}$	-
ANA_43	Et(Ind)2ZrCl2	**600**	30	-	**60**	9		$2,70x10^{-6}$	-
ANA_46	n-BuCpZrCl2	**600**		-	**60**	9		$2,72 \times 10^{-6}$	

APPENDIX 3 – mathematical description of deconvolution model [8]

The Mass weight distribution made with single site catalyst is described by Flory-Schluz most probable distribution.

Although were not considered transfer actions on kinetic models, for this model its need to consider all transfer reactions, once are this reactions responsible for broading the MWD.

If we consider the transfer to monomer reaction, which is the most significate in this present case, the population balance in steady state for to monomer free active site after transfer to monomer (P0) or chain with zero monomer is given by equation 4.9.

$$\frac{dP_0}{dt} = k_{tm}[M]Y_0 - k_p[M]P_0 - \frac{P_0}{t_R} \qquad (5.1)$$

Solving P_0 in order to Y_0 we have,

$$P_0 = \frac{\frac{k_{tm}[M]}{kp[M]}}{1+\frac{1}{k_p[M]t_R}} Y_0 \cong \frac{k_{tm}[M]}{kp\,[M]} Y_0 = \tau Y_0 \qquad (5.2)$$

T is the ratio between the chain transfer reactions and monomer propagation.

If we continue to do the same for the case that monomer 57ength57r with chain 57ength of 1 we obtain equation 5.1

$$\frac{dP_1}{dt} = k_p[M](P_0 - P_1) - k_{tm}P_1 - \frac{P_1}{t_R} \cong \frac{1}{1+\tau} P_0 \qquad (5.3)$$

If it´s solve in order to Pr we obtain equation 5.2

$$P_r = (\frac{1}{1+\tau})^r P_0 \qquad (5.4)$$

In this case we can do the previous approximation.

$$(\frac{1}{1+\tau})^r \cong e^{-r\tau} \qquad (5.5)$$

To obtain mass weight from the number of chain length distribution the transformation of equation 5.4 is needed.

$$w_r = \frac{rf_r}{\int_0^\infty rf_r dr} = r\tau^2 e^{-r\tau} \quad (5.6)$$

Since the usual to report MWDs measured by GPC is in logarithmic scale, flory distribution needs a transformation of variable given by equation 5.5

$$d\log r = \frac{\log e}{r} dr \quad (5.7)$$

$$w_{\log r} = 2{,}3026 \times r w_r \quad (5.8)$$

To obtain MWD we simply substitute MW= r x mw, where the mw is the average molar mass of the repeating unit in the polymer chain.

At the end the flory mass weight distribution in logarithmic scale is given by equation 5.7

$$w_{\log MW} = 2{,}3026 \times MW^2 \hat{\tau}^2 \exp(-MW\hat{\tau}) \quad (5.9)$$

Where,

$$\hat{\tau} = \frac{1}{Mn} \quad (6.0)$$

The simulation of model was run in an excel file provided by Prof. Dr. João B. P. Soares and Prof. Dr. Timothy F. L. Mckenna.

APPENDIX 4 – Results of fitting experimental data to origin equation (logistic function)

The curve get with this function have S-shaped and are typical to describe sigmol dose-response relationship.

$$Pressure\ (bar) = A_2 + \frac{(A_1 - A_2)}{1 + (\frac{t}{X_0})^p}$$

ANA_34 (n-BuCp 200ºC)

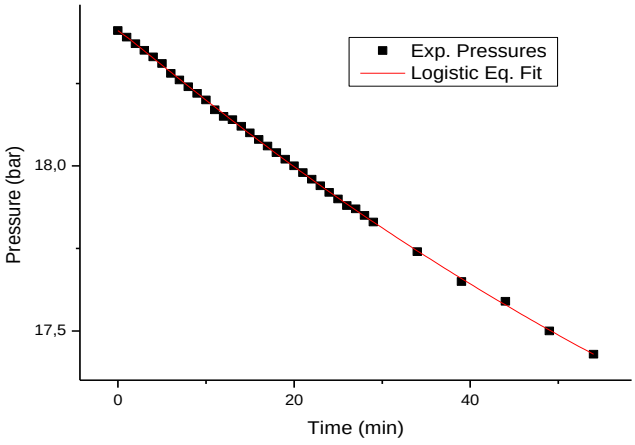

Parameters	Value	Standard Error
A1	18,41	0
A2	14,48	0,2934
x0	153,96	16,17
p	1,05	0,0131

Number of Points	35
Degrees of Freedom	32
Reduced Chi-Sqr	1,69E-05
Residual Sum of Squares	5,40E-04
Adj. R-Square	0,9997
Fit Status	Succeeded(100)

ANA_32 (n-BuCp 200ºC)

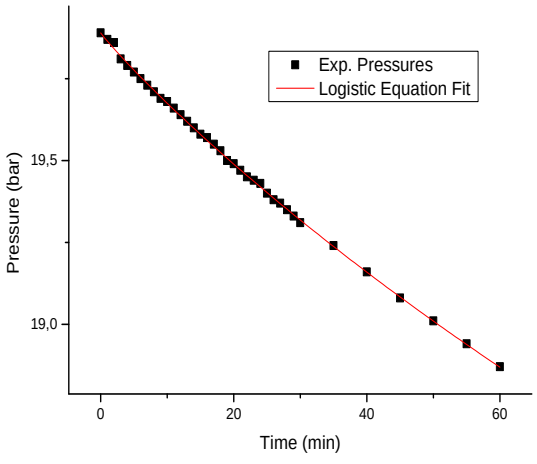

Parameters	Value	Standard Error
A1	19,89	0
A2	12,73	1,475
x0	405,59	116,1
P	0,9388	0,0169

Number of Points	37
Degrees of Freedom	34
Reduced Chi-Sqr	3,55E-05
Residual Sum of Squares	0,0012
Adj. R-Square	0,9994
Fit Status	Succeeded(100)

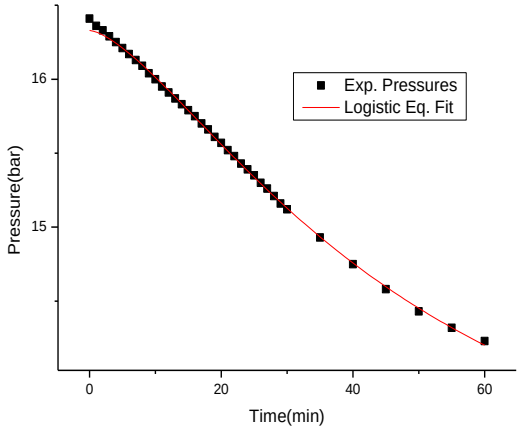

Parameters	Value	Standard Error
A1	16,33	0
A2	12,62	0,1574
x0	49,19	2,748
P	1,488	0,0330

Number of Points	36
Degrees of Freedom	33
Reduced Chi-Sqr	2,57E-05
Residual Sum of Squares	8,49E-04
Adj. R-Square	0,9999
Fit Status	Succeeded(100)

ANA_42 (EtInd2 450ºC)

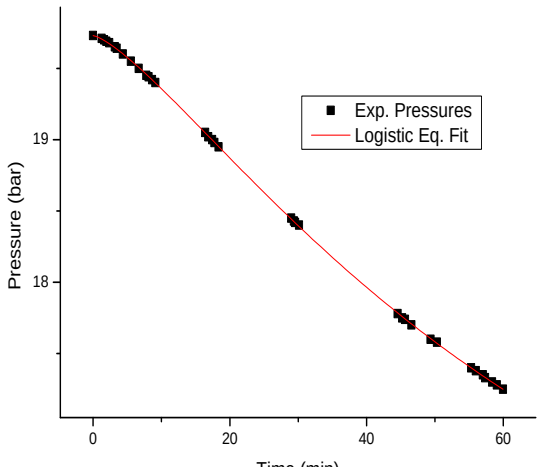

Parameters	Value	Standard Error
A1	19,73	0
A2	14,06141	0,0829
x0	72,30188	1,42241
p	1,3404	0,00717

Number of Points	37
Degrees of Freedom	34
Reduced Chi-Sqr	3,89E-04
Residual Sum of Squares	0,0132
Adj. R-Square	0,9988
Fit Status	Succeeded(100)

ANA_27 (n-BuCp 450ºC)

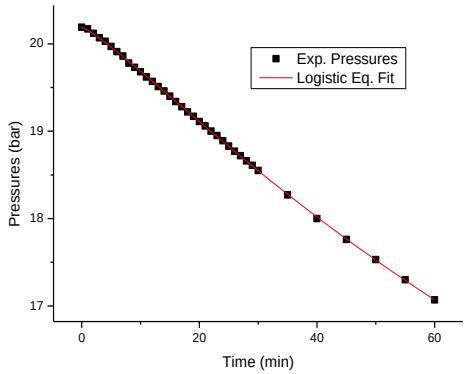

Parameters	Value	Standard Error
A1	20,19	0
A2	9,54	0,3931
x0	126,3	6,058
p	1,184	0,0086

Number of Points	37
Degrees of Freedom	34
Reduced Chi-Sqr	6,53E-05
Residual Sum of Squares	0,0022
Adj. R-Square	0,9999
Fit Status	Succeeded(100)

ANA_30 (n-BuCp 450ºC)

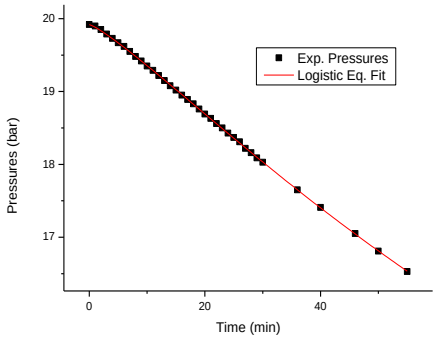

Parameters	Value	Standard Error
A1	19,92	0
A2	6,679	0,5133
x0	134,1	6,427
p	1,199	0,0078

Number of Points	36
Degrees of Freedom	33
Reduced Chi-Sqr	5,82E-05
Residual Sum of Squares	0,0019
Adj. R-Square	0,9999
Fit Status	Succeeded(100)

ANA_24 (EtInd2 600ºC)

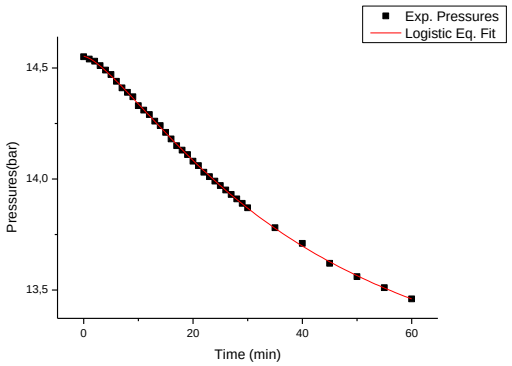

Parameters	Value	Standard Error
A1	14,55	0,0027
A2	12,82	0,0309
x0	40,62	1,024
p	1,391	0,0196

Number of Points	37
Degrees of Freedom	33
Reduced Chi-Sqr	1,98E-05
Residual Sum of Squares	6,53E-04
Adj. R-Square	0,9997
Fit Status	Succeeded(100)

ANA_43 (EtInd2 600ºC)

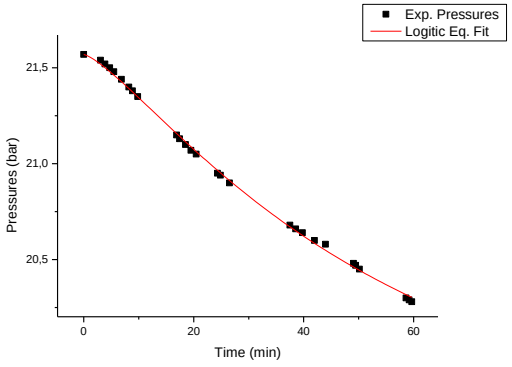

Parameters	Value	Standard Error
A1	21,57	0
A2	19,10	0,1816
x0	57,16	6,133
p	1,315	0,0462

Number of Points	28
Degrees of Freedom	25
Reduced Chi-Sqr	2,68E-04
Residual Sum of Squares	0,00669
Adj. R-Square	0,9985
Fit Status	Succeeded(100)

APPENDIX 5 – Mass of ethylene

I - MESURE DE SOLUBILITE.

1 - Masse volumique de l'éthylène :

Ces données sont connues dans un large domaine de températures (- 50 + 150°C) et de pressions (1 - 1500 bars) (100) (Fig. 1).

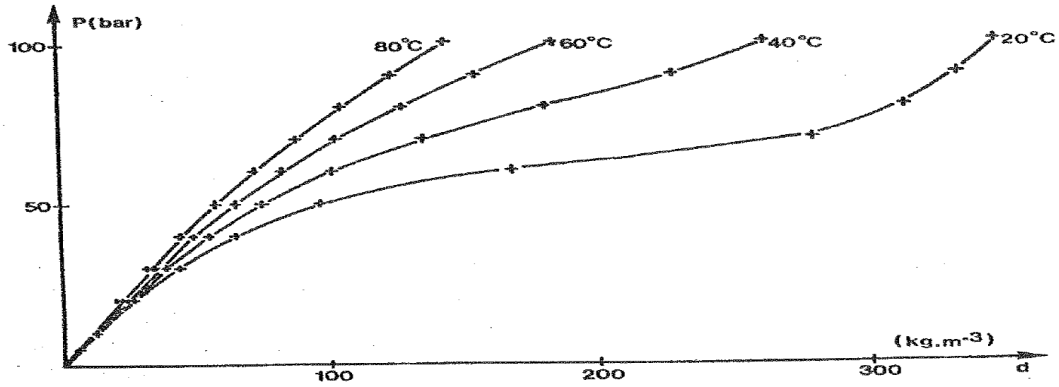

Figure 1 - Masse volumique de l'éthylène (100).

Pour interpoler entre les points expérimentaux, nous avons établi par régression parabolique, dans le domaine que nous utilisons, une loi de la forme :

$$d = \delta(P, T)$$

(1) $$d = (\alpha_0 + \alpha_1 t + \alpha_2 t^2) + (\alpha_3 + \alpha_4 t + \alpha_5 t^2) P + (\alpha_6 + \alpha_7 t + \alpha_8 t^2) P^2$$

pour $1 \text{ bar} < P < 80 \text{ bars}$

$15°C < t < 105°C$

Elle est établie de la façon suivante :

à chaque température donnée, par régression parabolique, on établit :

$$d = a_o + a_1 P + a_2 P^2 \text{ pour } 0 < P < 80 \text{ bars}$$

Pour augmenter la précision de la régression, on n'a pas utilisé les masses volumiques réelles mais leur quotient par la pression, ce qui ramène toutes les valeurs au voisinage de l'unité. On peut considérer le terme ainsi défini comme une densité. Puis, à chaque température, correspond un coefficient α_o, α_1 ou α_2, ces derniers sont mis sous la forme :

$$a_o = \alpha_o + \alpha_1 t + \alpha_2 t^2$$

$$a_1 = \alpha_3 + \alpha_4 t + \alpha_5 t^2 \ldots\ldots$$

On obtient :

$$a_o = 1,256 - 4,505.10^{-3}\ t + 1,090.10^{-5}\ t^2$$
$$a_1 = 5,2.10^{-3} - 1,495.10^{-5}\ t - 1,244.10^{-7}\ t^2$$
$$a_2 = 3,252.10^{-4} - 7,32.10^{-6}\ t + 4,195.10^{-8}\ t^2$$

Cette formule est programmée sur machine et on obtient instantanément la masse d'éthylène contenue dans un volume donné, à pression et température fixées.

L'utilisation de ces coefficients permet de retrouver les points expérimentaux à partir desquels la régression a été faite avec une erreur de 0,5 % au plus.